The effect of *Sclerotinia sclerotiorum* infection on *Cannabis sativa*

by

Natalie L. Cale

A thesis submitted to the Faculty of Graduate Studies of

The University of Manitoba

in partial fulfillment of the requirements of the degree of

MASTER OF SCIENCE

Department of Biological Sciences

University of Manitoba

Winnipeg, Manitoba, Canada

ABSTRACT

Known to infect more than 600 plant species worldwide, *Sclerotinia sclerotiorum* is a necrotrophic fungal pathogen, and the causative agent of white mold. With recent infection reports documented across North America, *Cannabis sativa* is known to be susceptible to *Sclerotinia* infection. Resulting from legal constraints associated with *C. sativa*, little is known about the *Cannabis*-*Sclerotinia* pathosystem, particularly in how the plant responds to pathogen attack at the cellular and molecular levels. Our anatomical study revealed initial infection and degradation of the epidermis and cortical parenchyma, followed by widespread infection of the vascular phloem. Dual RNA sequencing of the *C. sativa* cola provided a detailed transcriptomic profile of this pathosystem directly at the site of infection over time. Differential gene expression analysis revealed large-scale transcriptional shifts resulting from rapid infection. Gene ontology term enrichment identified processes associated with plant defense and signal transduction cascades during *C. sativa* infection while processes associated with redox control and sugar catabolism were enriched in the *S. sclerotiorum* pathogen. Taken together, this study revealed transcriptional reprogramming in both the host plant and fungal pathogen associated with floral infection in space and time.

ACKNOWLEDGEMENTS

I would like to thank several people who have helped make my graduate program such a positive experience and without whom I would not have been able to complete my MSc. I would first like to express my profound gratitude to my supervisor, Dr. Mark Belmonte, for his guidance and all that he has done for me over the course of my MSc. Mark is an incredible leader and person, and I am so grateful to have had the opportunity to have studied as a member of the Belmonte lab. His mentorship has not only bettered me as a scientist, but also as an individual. I also owe many thanks to my thesis committee members, Dr. Steve Whyard and Dr. Jae-Hyeok Lee. Thank you both for agreeing to be a part of my committee, and for your insight throughout the course of my graduate program. I wish to thank all members of the Belmonte Lab, both past and present, for making the lab such an amazing environment to be a part of. I would specifically like to thank Dr. Bliss Beernink, Dr. Dylan Zeigler, Dr. Phil Walker, Dr. Nick Wytinck, Rylee Swiderek, Haben Tesfu and Yujia Wu for their time and ideas. I would also like to thank Sean Robertson for the computational insight and guidance he was able to provide to my project. Additionally, this project would not have been possible without the help of Noel Galuschik, the University of Manitoba's Cannabis and Security Research Officer, and of Rogue Botanical who provided us with the plants used in this thesis. Lastly, I would like to extend my sincere thanks to my family and friends, my parents, and my partner, Brett, for their encouragement over the past few years. Thank you all for providing your continual support, and for your patience when my attention was required on my studies. I appreciate you all and am immensely grateful for the opportunities this program has afforded me.

TABLE OF CONTENTS

LIST OF FIGURES

LIST OF SUPPLEMENTARY FIGURES

NON-COMMON ABBREVIATIONS

CWDE	Cell wall degrading enzymes
DAMP	Damage associated molecular pattern
DEG	Differentially expressed gene
dpi	Days post inoculation
ETI	Effector triggered immunity
FDR	False discovery rate
GO	Gene ontology
HR	Hypersensitive response
ISR	Induced systemic resistance
JA	Jasmonic Acid
MRL	Maximum residual level
NLR	Nucleotide-binding leucine-rich repeat
PAL	Phenylalanine ammonia lyase
PAMP	Pathogen associated molecular pattern
PCA	Principal component analysis
PG	Polygalacturonase
PR	Pathogenesis related
PRR	Pattern recognition receptor
PTI	Pattern triggered immunity
REDOX	Oxidation-reduction
RLK	Receptor-like kinase
ROS	Reactive oxygen species

SA	Salicylic acid
SAR	Systemic acquired resistance
WAK	Wall associated kinase
WAKL	Wall associated kinase-like

CHAPTER ONE: Introduction

Cannabis sativa

Cannabis sativa L. (hereafter referred to as *Cannabis or C. sativa)* is believed to have originated in Central Asia (Long et al., 2017; Ren et al., 2021) and remains one of the most widely cultivated, yet controversial plants grown around the world (Braich et al., 2019). Grown for its fibre, medicinal, and psychoactive properties, *Cannabis* quickly spread throughout Asia and Europe, and today is grown and sold internationally both legally and illegally (van Bakel et al., 2011). *C. sativa* is an annual, wind-pollinated, diploid (2n = 20) flowering plant species. It is also dioecious, and is one of few plant species to use an XY chromosomal system of sex differentiation, with a male determining Y (Divashuk et al., 2014; Ren et al., 2021). *Cannabis* flowering is tightly regulated by photoperiod, with cultivar-specific optima usually within the range of ~12-15 hours (M. Zhang et al., 2021). Thus, photoperiod is often manipulated by commercial growers to induce flowering and obtain high seasonal yields over multiple crop rotations (Small, 2015).

As a dioecious plant species, *C. sativa* produces both pistillate and staminate flowers in female and male plants, respectively (Leme et al., 2020). As female plants are grown for "drug-type" *Cannabis*, they will be the focus of this thesis. Female *C. sativa* flowers aggregate closely together to form inflorescences, which are densely clustered at the apex of plant branches to form a structure often informally referred to as the "cola" (Raman et al., 2017). Individual flowers consist of an ovary and style which lead to a pair of stigmas that extend from the enveloping bract of the flower (Leme et al., 2020; Raman et al., 2017). Covering the surface of the female bracts are resin-containing secretory glandular trichomes. The biosynthesis and storage of

cannabinoids and many terpenes occurs within secretory glandular trichomes of the female *C. sativa* flowers (Booth et al., 2017; Rodziewicz et al., 2019; Xie et al., 2023). As the flowers are the region of highest glandular trichome density, and thus cannabinoid/terpene-containing resin, it is the cola or inflorescences of the plant that are harvested for retail drug sale.

The classification of species within the *Cannabis* genus has historically been controversial. Some claim the genus contains three species (*C. sativa*, *C. indica* and *C. ruderalis*), whereas others hold a more widely accepted opinion, that the genus is monotypic, and that observable subpopulations are subspecies of *C. sativa* (de Meijer et al., 2003; Hillig, 2005; Hurgobin et al., 2021; Sawler et al., 2015). With the uncertainty and dispute surrounding the taxonomic classification of the *Cannabis* genus, we use the monotypic definition of *C. sativa* in this study. Furthermore, *C. sativa* describes plants grown both as industrial hemp and plants grown as marijuana. Hemp (or "fibre-type" *Cannabis*) and marijuana ("drug-type" *Cannabis*) have been given different definitions based either on a threshold concentration of Δ^9-tetrahydrocannabinolic acid (THCA) cannabinoid content or based on their chemical phenotype, referred to as chemotype. Plants deemed "fibre-type" contain THCA levels lower than 0.3% dry weight, whereas plants with >0.3% THCA are considered as "drug-type" in regulations set by the governments of Canada, the European Union and the United States (Ren et al., 2021). On the other hand, chemotype classification of *Cannabis* involves classifying plants based on the ratio of THCA to cannabidiolic acid (CBDA) present in tissues, where hemp typically produces higher concentrations of CBDA than THCA, and "drug-type" cannabis produces very high amounts of THCA compared to CBDA (de Meijer et al., 2003; Hurgobin et al., 2021; Ren et al., 2021). THCA and CBDA are examples of psychoactive and non-psychoactive cannabinoids found

within the secretory cavity of glandular trichomes. In addition to cannabinoids, the resin found within glandular trichomes contains high levels of mono- and sesquiterpenes which are responsible for the scent/flavour of *C. sativa* flowers and products, influencing consumer product selection (Booth et al., 2017; Booth & Bohlmann, 2019; Fischedick, 2017). The *C. sativa* studied in this thesis is of the cultivar 'Kona', which is considered to be "drug-type". Given 'Kona' falls under the "drug-type" of *C. sativa*, the plants used in this study were grown under a Health Canada research permit in collaboration with the University of Manitoba and Rogue Botanical, the supplier of the plants.

Diseases of *Cannabis sativa* and available control measures

In October of 2018, Canada became the second country to legalize *C. sativa,* after Uruguay, for non-medical use and retail sale (Government of Canada, 2018; Hammond et al., 2020). As *Cannabis* demand increases internationally, governing health and safety bodies continue to develop regulatory practices aimed at ensuring quality and safety of *Cannabis* products for users (Craven et al., 2019). Analytical testing of *Cannabis* products generally includes testing for microorganisms and mycotoxins, heavy metals and active ingredients in pesticide/fungicides. Regulations specific to allowable limits, specifically of pesticide/fungicides in *Cannabis,* vary considerably between regional governing agencies. For instance, the state of Oregon in the United States mandates testing for 59 pesticides, whereas testing for 96 pesticide active ingredients is federally mandated in Canada (Craven et al., 2019). Furthermore, the maximum residual levels (MRLs) of the above-mentioned pesticides vary considerably between countries/states, while Canada has currently implemented stricter controls on pesticides detected in *Cannabis* products than the United States. Further, due to legal constraints associated with *C.*

sativa around the world, in addition to its classification as a Schedule 1 narcotic in the United States, limited research can be conducted for the purpose of establishing pesticide tolerances (Goldman et al., 2021; Sandler et al., 2019). While MRLs for *Cannabis* remain considerably low, notably in the Canadian market, producers rely on cultural and biological control practices for successful *Cannabis* production (Lemay et al., 2022; Sandler et al., 2019). As surpassing acceptable MRLs requires destruction of harvested *Cannabis* product, there is an immediate need to develop novel crop protection strategies to protect *C. sativa* against pathogens and pests.

As of March 2024, the registered growing area for *Cannabis* in Canada was reported at 1.39 and 6.24 million m^2 of indoor and outdoor growing area, respectively (Government of Canada, 2024). With extensive indoor and outdoor cultivation, emerging diseases of *C. sativa* have been reported in recent years. Plant diseases in *C. sativa* have been documented to affect various tissues including roots, stems and foliage, and inflorescences both pre- and postharvest (Punja, 2021; Sirangelo et al., 2023). The majority of pathogens known to infect *C. sativa* are of fungal origin, while viroid/viruses remain a concern to producers (Punja, 2021). In comparison, bacterial infection of *C. sativa* is infrequently reported, resulting in reduced producer concern. Major fungal pathogens of *C. sativa* include various *Fusarium* species (*F. oxysporum, F. proliferatum,* and *F. solani*), *Golovinomyces* spp.*,* and *Botrytis cinerea*, with specific details of symptom development resulting from each pathogen available in a review article by Punja (2021). More recently, *Sclerotinia sclerotiorum* has been reported to have infected *C. sativa* both in field and greenhouse conditions across North America, and has been reported as a pathogen of emerging concern for both the medicinal *Cannabis* and industrial hemp industries (Bains et al., 2000; Garfinkel, 2021; Punja, 2021; Punja & Ni, 2021; Thiessen et al., 2020; Yang et al., 2023).

Symptoms listed in the infection reports of Bains et al. (2000), Garfinkel (2021) and Yang et al. (2023) highlight the development of friable tan/brown necrotic cankers and lesions developing on the crown, along the stem, and within the inflorescence of plants. Also documented in these reports was the presence of white mycelium, and sclerotia present at the site of the lesion, as well as within the pith cavity of the stem. Although *S. sclerotiorum* infection reports have been documented, this interaction has yet to be described at the cellular and molecular levels, and as a result will be the focus of my thesis.

Sclerotinia sclerotiorum **biology and lifecycle**

Sclerotinia sclerotiorum is a necrotrophic fungal pathogen responsible for the diseases of white mould, Sclerotinia stem rot and Sclerotinia stem canker, among more than 60 other names (Bolton et al., 2006; Purdy, 1979). Known to infect more than 600 plant species around the world including agricultural and horticultural crops, ornamentals, trees/shrubs and weed species, *S. sclerotiorum* is responsible for devastating yield losses every year in North America (Bolton et al., 2006; Liang & Rollins, 2018; Saharan & Mehta, 2008; Willbur et al., 2019). Found in various countries around the world, *S. sclerotiorum* is most commonly reported in areas with a temperate climate that leads to the development of high humidity conditions (Purdy, 1979; Saharan & Mehta, 2008). Although yield losses resulting from *S. sclerotiorum* infection vary considerably based on geographic location and crop species, losses in favourable conditions for infection are often reported at 20-35%, although losses over 50% and as high as 80-100% have been documented (Alkooranee et al., 2017; Hossain et al., 2023). *S. sclerotiorum* infection is difficult to control largely due to its rapid and aggressive disease progression in addition to its long-term persistence in the soil in the form of sclerotia. Sclerotia are dense melanized resting structures

resistant to physical and chemical degradation that allow *S. sclerotiorum* to overwinter in the soil (Bolton et al., 2006; Smolińska & Kowalska, 2018, 2018). As the primary surviving fungal structure, sclerotia remain dormant in the soil until sufficiently humid conditions allow for myceliogenic or carpogenic germination (Bolton et al., 2006; Hossain et al., 2023). Myceliogenic germination refers to direct host infection via mycelia, whereas carpogenic germination results in the production of apothecia and subsequent ascospore release to initiate infection. Mycelia originating from myceliogenic sclerotial germination may initiate infection of plant parts that are in contact with the soil such as roots and the basal stem or crown, whereas ascospore release may initiate infection on aerial plant parts (Ekins et al., 2002).

Upon landing on aerial parts of the host plant, *S. sclerotiorum* ascospores germinate to initiate infection (Figure 1). However, before infecting healthy plant tissues, germinated ascospores must first infect dead or senescing host tissues (Bolton et al., 2006; Girard et al., 2017; Hossain et al., 2023; Sutton & Deverall, 1983; Wytinck et al., 2022). To penetrate the physical barriers of the host plant such as the cuticle, *S. sclerotiorum* uses either simple appressoria or specialized complex appressoria known as infection cushions (Bolton et al., 2006; Girard et al., 2017; Hegedus & Rimmer, 2005; Hossain et al., 2023). Regarded as a highly aggressive pathogen, *S. sclerotiorum* has been shown to penetrate the *Brassica napus* (canola) leaf epidermis and mesophyll within 24 hours post inoculation (hpi) and the vasculature by 48 hpi (Girard et al., 2017; Walker et al., 2022). Once established in the host plant tissues, the fungus then initiates the true pathogenic phase of its infection cycle through the production of plant cell wall degrading enzymes (CWDEs) and oxalic acid (OA), among other effectors (Hegedus & Rimmer, 2005; Horbach et al., 2011). OA is known to be essential for *S.*

sclerotiorum pathogenicity as OA deficient mutant strains have been previously seen to exhibit poor pathogenicity (Godoy et al., 1990). Known to acidify the environment of the middle lamellae, OA also sequesters calcium, disrupts REDOX homeostasis, and increases activity of pectinolytic enzymes (Girard et al., 2017; Hegedus & Rimmer, 2005; K. S. Kim et al., 2008; Lumsden, 1976). This cascade results in cell death and necrotic lesion formation. Infection becomes systemic as the fungus spreads to the vasculature and eventually the pith thus degrading host plant tissues as the fungus travels through the body of the plant (Derbyshire & Denton-Giles, 2016; Wytinck et al., 2022). Due to the rapid attack and degradation of host plant tissues by *S. sclerotiorum*, the plant immune response is generally insufficient to defend against infection (Wytinck et al., 2022).

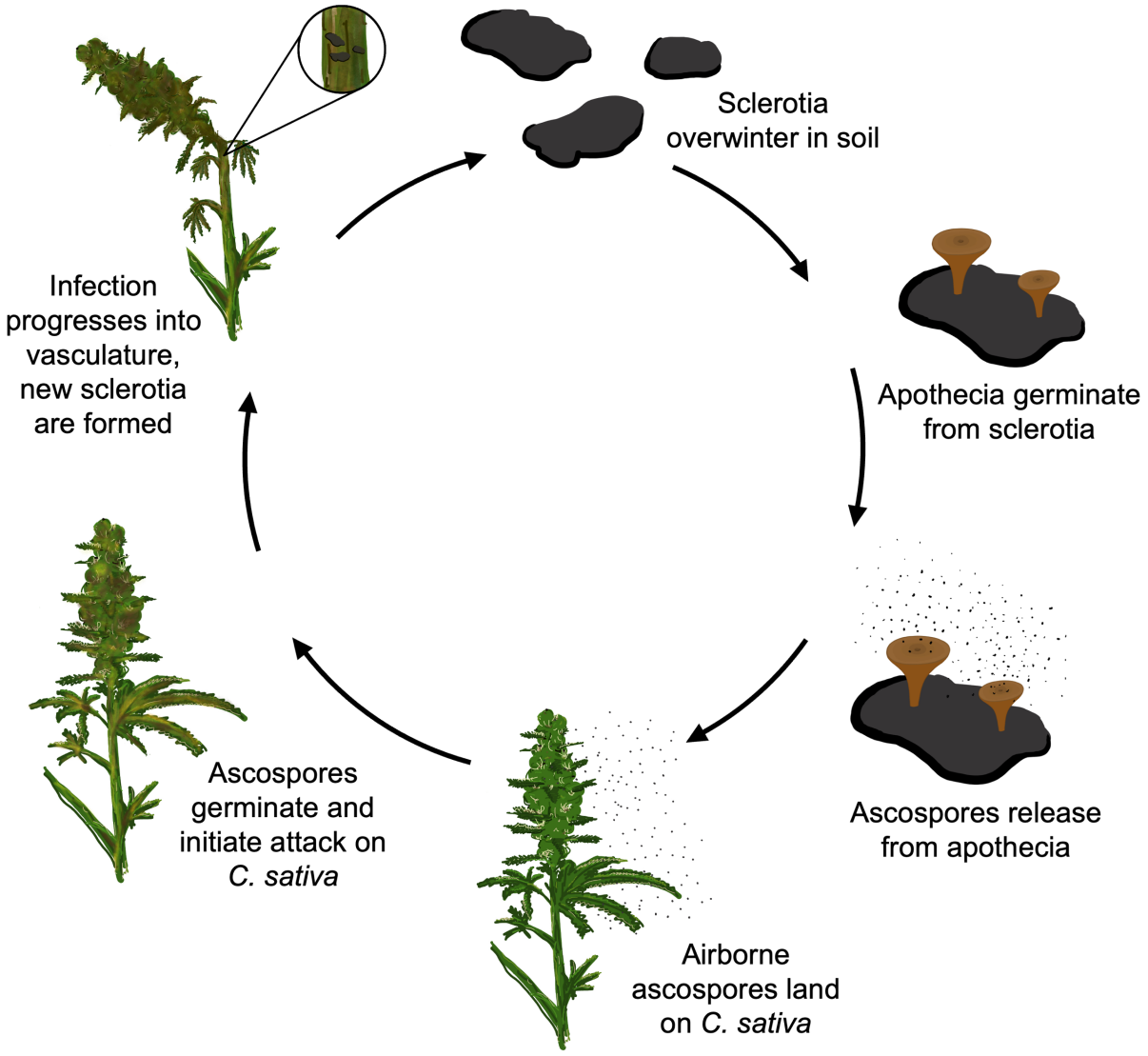

Figure 1. Hypothetical *S. sclerotiorum* lifecycle with *C. sativa*. Resting melanized sclerotia in the soil germinate to produce apothecia which in turn release ascospores. Airborne ascospores land on *C. sativa* and germinate upon landing on senescing tissues. As fungal mycelia establish and infection begins, tissue is necrotized, leading to the formation of lesions and soft rot. Hyphal growth progresses leading to eventual plant death and the production of new sclerotia.

Pathogen perception and the plant immune response

The contents of this section have been published (with some modifications) in Annals of Botany PLANTS https://doi-org.uml.idm.oclc.org/10.1093/aobpla/plae056 (Cale et al., 2024).

Plants have evolved complex mechanisms to defend themselves upon pathogen attack. As such, the host plant response to pathogenic fungi relies on a variety of signalling processes and resistance/immunity pathways. For example, activation of the innate immune system occurs when the presence of a pathogen is recognized through extracellular pathogen-associated molecular patterns (PAMPs). Fungal pathogens such as *S. sclerotiorum* are also detected via pattern recognition receptors (PRRs), specifically receptor protein kinases (RLKs), or through the detection of pathogen effectors via nucleotide-binding leucine-rich repeat (NLR) receptors (Song et al., 2021). Recognition of PAMPs via PRRs elicit pattern triggered immunity (PTI), whereas recognition of pathogen effectors via NLRs elicit effector triggered immunity (ETI). It is generally accepted that PTI confers a lower-level of immunity effective against non-adapted pathogens whereas ETI is more effective against host-adapted pathogens as its associated immunity is more robust (Pruitt et al., 2021). However, more recently it has been found that the two immune pathways are not found to be mutually exclusive, with co-induction having led to increased pathogen resistance, and PTI even having been found to be necessary for a successful immune response as a result of ETI (Pruitt et al., 2021; Walker et al., 2022). Following pathogen recognition, early defense responses are initiated such as signal transduction and mitogen-activated protein kinase (MAPK) cascades, which in turn lead to calcium ion import, reactive oxygen species (ROS) burst, and regulation of phytohormone signalling pathways that allow for defense gene induction (Song et al., 2021; Walker et al., 2022; Wytinck et al., 2022).

Following a targeted immune response, plant systemic resistance may be attained via two discrete pathways: i) systemic acquired resistance (SAR) and ii) induced systemic resistance (ISR). When SAR is induced, areas distal from the infection site take on a heightened immune state, undergoing largescale transcriptional changes that leave them primed for a more rapid and robust response following pathogen infection (Jung et al., 2009; Zeier, 2021). SAR activation is often characterized by increased levels of the defense hormone, salicylic acid (SA), in addition to increased pathogenesis-related (PR) protein expression systemically (Bernsdorff et al., 2016; Pieterse et al., 2014). While increased systemic resistance to pathogen attack is also seen as a result of induced ISR, the two resistance pathways operate through distinct mechanisms. While ISR is seen to be effective without the accumulation of PR proteins, it is also mediated in a SA-independent signalling pathway, instead relying on jasmonic acid (JA) as a primary signalling hormone (Pieterse et al., 2014). Additionally, ISR is commonly seen to be initiated through interactions with plant roots by non-pathogenic rhizobacteria or fungi, or in response to insect herbivory, whereas SAR is commonly activated following pathogen attack or as a result of defense-response related molecules/hormones (Duke et al., 2017; Pieterse et al., 2014).

Research objectives

Due to legal constraints associated with working with *C. sativa,* the plant remains relatively understudied today. As *C. sativa* legalization expands, along with the international growth of the crop, there is an increased need for strategies to protect *C. sativa* from fungal pathogens like *S. sclerotiorum*. With MRLs specific to *Cannabis* products restricting producers' options to protect their crops, there is an immediate need to understand the molecular mechanisms underpinning

the *C. sativa – S. sclerotiorum* pathosystem. Data gained from this research will provide a valuable resource for those interested in understanding and developing novel genetic strategies to protect this commercial crop. The overall objective of my research is to characterize the infection of the *C. sativa* cola at the transcriptomic and anatomical levels. Exploring this interaction at both the host plant and fungal pathogen levels will provide novel insight into this pathosystem.

Research questions and hypotheses

Global transcriptomic profiling of the *C. sativa-S. sclerotiorum* pathosystem

Questions: How do the expression of genes underpinning the C. sativa – S. sclerotiorum pathosystem change during the course of infection in the cola?

I hypothesize that both *C. sativa* and *S. sclerotiorum* will show large-scale transcriptomic changes as a result of infection. I hypothesize that in response to infection, *C. sativa* will activate genes involved in plant SAR and ISR pathways, along with changes in hormone crosstalk. In *S. sclerotiorum*, I hypothesize that differential gene expression analysis will reveal induction of genes involved in plant cell wall degradation and toxin biosynthesis throughout the infection cycle.

Anatomical study of the *C. sativa-S. sclerotiorum* pathosystem

Question: How does S. sclerotiorum initiate infection of the C. sativa inflorescence? How does fungal infection spread throughout the C. sativa cola?

I hypothesize that *S. sclerotiorum* hyphae will rapidly extend from the mycelial inoculant plug and spread over the epidermis prior to penetrating into host parenchymatous tissues. Upon penetration of host plant tissues, I expect to see degradation of the epidermis and

mesophyll/cortex/parenchymatous tissues before travelling into the plant's vasculature. Once in the vasculature, I expect to see further expansion within the main stem of the plant by way of the vasculature, accompanied by extensive cell wall degradation that follows the proliferating pathogen.

CHAPTER TWO: Materials and methods

Cannabis sativa growth conditions

Female *C. sativa* plants, cultivar 'Kona' were sourced from Rogue Botanical, a licensed grower in southern Manitoba, Canada. Plants were obtained in vegetative growth, 20 days after being clonally propagated. At 22 days old, plants were transplanted from 4-inch pots to 6-inch pots in Sunshine growing mix #4 (Sungro, Agawan, MA, USA). Plants were grown in a controlled environment chamber under long day conditions (18h light, 6h dark), light settings of 500 μmol/m^2/s^{-1}, 23°C and 50% relative humidity. After 30 days in vegetative growth, the photoperiod was adjusted to 12h light, 12h dark to promote flowering. Plants were fertilized using Advanced Nutrients Sensi Grow/Bloom nutrient packages, as per manufacturer's instructions (Advanced Nutrients, West Hollywood, CA, USA).

Sclerotinia sclerotiorum inoculation of the *Cannabis sativa* cola

S. sclerotiorum was grown *in vitro* on potato dextrose agar (BD Difco) plates supplemented with 15 μg/mL tetracycline HCl. *S. sclerotiorum* mycelial plugs were taken from the leading edge of a 3-day-old actively growing plate using a P1000 pipette tip. Mycelial plugs were carefully placed at the inflorescence node of the third-most distal inflorescence of the *C. sativa* cola using forceps. Infection took place over a seven-day period with colas being harvested after 1-, 3-, 5- and 7- days post inoculation (dpi). Both infected and untreated control (UTC) colas were harvested at each timepoint.

Sample collection, RNA isolation, library preparation and RNA sequencing

Harvested colas were immediately trimmed down to the main floral stem, while maintaining ~1 cm^3 of floral tissue of the inoculated inflorescence and immediately flash frozen using liquid nitrogen. Tissue was ground to a fine powder using a mortar and pestle using liquid nitrogen prior to RNA extraction.

RNA was extracted using the Purelink Plant RNA Reagent (Invitrogen, Waltham, MA, USA) as per manufacturer's protocol. Following RNA extraction, Qiagen's RNeasy Plant Minikit and RNase-Free DNase Set was used for DNAse treatment following the "RNA Cleanup" protocol available in Qiagen's RNeasy Mini Handbook (Qiagen, Toronto, ON, Canada). As sample purity was often compromised as a result of the DNAse treatment procedure, samples then underwent a sodium acetate precipitation. This precipitation used 3M $C_2H_3NaO_2$ (pH 5.2) and subsequent ethanol washes (100% followed by 75%) before resuspension in molecular grade water to yield RNA of increased purity.

cDNA libraries were constructed by Genome Québec following their polyA Enriched RNA Library Preparation protocol. Paired-end 100 base pair reads were sequenced for a minimum of 25 million reads per library on the Illumina NovaSeq sequencing system at Genome Québec (Montréal, Québec, Canada). All sequencing data can be found at the Gene Expression Omnibus, under accession GSE284432.

RNA-seq analysis

Raw reads were processed using computing clusters available through Compute Canada and the Digital Research Alliance of Canada (www.aliancecan.ca). Prior to read alignment,

sequence read quality was first assessed using FastQC (Andrews, 2010). Paired-end read alignment was carried out using the *C. sativa* cultivar 'Pink Pepper' reference genome (NCBI RefSeq assembly GCF_029168945.1; Lim, 2023) and the *S. sclerotiorum* reference genome (NCBI RefSeq assembly GCF_000146945.2; Amselem et al., 2011) using HISAT2 (Kim et al., 2019). Transcript abundance was determined using featureCounts (Liao et al., 2014).
With one of the barriers to working with the *C. sativa* transcriptome being the level of genome annotation, we used predicted protein orthologs publicly available for the loci of the *C. sativa* cultivar 'Pink Pepper' genome through the NCBI Genomes database (RefSeq accession GCF_029168945.1; Lim, 2023). Differential gene expression analysis, low counts filtering, library normalization, principle component analysis and further data visualization was done using libraries DESeq2 (Love et al., 2014), ashr (M. Stephens, 2017), and ggplot2 (Wickham, 2011) in R (R Core Team, 2021). Genes with counts lower than 10 across all samples were filtered prior to normalization and differential gene expression analysis. Raw sequenced read counts were normalized using the median of ratios method in DESeq2 (Anders & Huber, 2010). Differentially expressed genes (DEG) were called with a p-value < 0.01 when adjusted for false discovery rate (FDR) by the Benjamini-Hochberg method (Benjamini & Hochberg, 1995). Gene ontology (GO) term enrichment was carried out on differentially expressed gene sets using SeqEnrich (Becker et al., 2017).

Sample preparation for light microscopy

Sample preparation, sectioning and staining followed the methods previously described by Chan and Belmonte (2013) with slight modifications. Harvested colas were trimmed to the above-mentioned region of interest before being fixed in a solution of 2.5% glutaraldehyde and

1.6% paraformaldehyde in 1x phosphate-buffered saline. Tissue was added to fixative solution before being vacuum infiltrated for 30 minutes to ensure adequate penetration of the fixative into the *C. sativa* tissues. Tissue samples were fixed for 24 hours at 4°C. Tissue was decoloured in methyl cellosolve for 24 hours, followed by daily 100% ethanol changes for three days at 4°C. Historesin (Leica Microsystems, Wetzlar, Germany) was gradually infiltrated into processed tissue using a 30%, 50%, 75% and 100% ethanol: historesin mixture. Pure Historesin was exchanged three times over the course of a week, while vacuum infiltrating the tissue in for 30 mins halfway through this period. Tissue was then embedded in round molds using an embedding medium composed of 91.5% Historesin, 2.4% polyethylene glycol 400, and 6.1% Historesin Hardener (Leica Microsystems, Wetzlar, Germany; Chan & Belmonte, 2013).

Sectioning and staining for light microscopy

Hardened Historesin blocks were sectioned at 3 µm using disposable Epredia Edge-Rite steel blades (Epredia, Kalamazoo, MI, USA) mounted on a Leica RM2245 microtome (Leica Microsystems, Wetzlar, Germany). Sections were placed on glass slides for staining.

Sections were first stained with periodic acid-Schiff stain (15 minutes in 0.1% periodic acid, followed by 15 minutes in Schiff's reagent) before being stained with 0.1% toluidine blue O suspended in distilled water for 30 seconds. Following staining, coverslips were mounted on the slides using Cytoseal 60 (Richard-Allen Scientific, Kalamazoo, MI, USA). Slides were viewed using a brightfield light microscope and micrographs were taken using the Leica Application Suite software version 4.6.0 (Leica Microsystems, Wetzlar, Germany). Image

cropping and the addition of scale bars was carried out in Adobe Photoshop version 25.7.0 (Adobe Systems Inc., San Jose, CA, USA).

CHAPTER THREE: Results

S. sclerotiorum initiates rapid infection in *C. sativa* floral tissue

First, we performed *S. sclerotiorum* infection assays of the *C. sativa* cola to better understand disease progression over time (Figure 2). At one day post inoculation (dpi) no external disease symptoms were visible on the cola (Figure 2A, i-iii). At 3 dpi, we first observed floral tissue necrosis at the site of inoculation (Figure 2A, iv). By 5 dpi, necrosis was observed throughout the inoculated inflorescence and had extended to the inflorescence axis, nearing the main stem of the cola (Figure 2A, v). Finally, at 7 dpi, necrosis had become widespread, affecting neighbouring inflorescences of the cola and had extended down into the main stem axis (Figure 2A, vi). Infected necrotized tissues were pale brown in colour, and friable. Necrotic tissue present in the interior of the cola was soft and water-soaked, while necrotic tissue found towards the exterior of the cola was dry and brittle. Alignment of RNA sequencing reads to both the *C. sativa* and *S. sclerotiorum* genomes revealed similar trends, where percent alignment to *S. sclerotiorum* increased in infected samples as time post inoculation progressed, while the opposite trend was observed for reads aligned to the *C. sativa* genome (Figure 2B).

Global shifts in gene expression were observed in both the host plant and fungal pathogen as *S. sclerotiorum* initiated infection in *C. sativa.* Hierarchical clustering analysis was used to determine levels of similarly between samples of different timepoints and infection statuses. Clustering the top 10,000 most variably expressed *C. sativa* genes revealed that treatments clustered together based on infection status with the exception of the 1 dpi timepoint which remained clustered with uninfected samples (Figure 2C). These results were supported by principal component analysis (PCA) of individual samples which revealed that the largest source

of variation in our data was attributed to infection status (Figure S1). Furthermore, infected samples clustered into distinct groups based on time post inoculation, highlighting large shifts in gene activity as infection progressed across the seven-day infection period. Similarly, hierarchical clustering of the top 1000 most variably expressed *S. sclerotiorum* genes revealed the 1 dpi timepoint to cluster with *in vitro* grown *S. sclerotiorum*, while all other infection timepoints clustered distinctly (Figure S2). PCA of individual samples directly supported hierarchical clustering results (Figures S3).

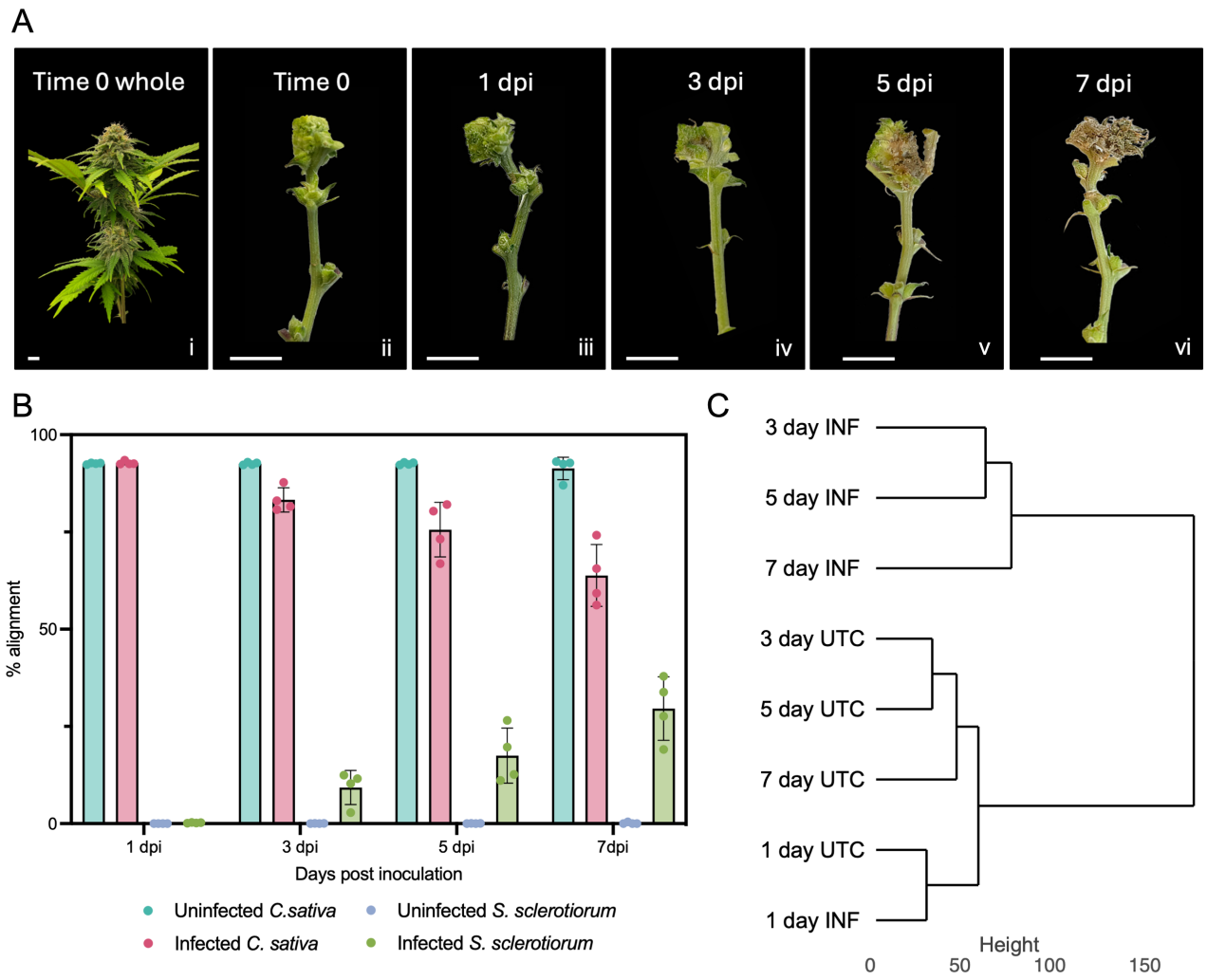

Figure 2. *S. sclerotiorum* infection of the *C. sativa* cola. (A) Symptom progression of *S. sclerotiorum* infection of the *C. sativa* cola up to seven days post inoculation (dpi). Whole cola (i) pictured next to trimmed cola (ii), both at time zero. Trimmed infected colas pictured at 1-, 3-, 5-, and 7 dpi indicated as iii, iv, v, and vi, respectively. Scale bar = 1 cm. (B) Percent alignment of RNA sequencing reads from infected and uninfected control samples to both the *C. sativa* and *S. sclerotiorum* genomes. Colour corresponds to infection status and the genome to which reads were aligned. (C) Dendrogram of *C. sativa* samples based off hierarchical clustering of the top 10,000 most variable genes. Height corresponds to Euclidean distance between clusters. INF = infected, UTC = untreated control.

S. sclerotiorum rapidly infects *C. sativa* tissues and preferentially infects phloem tissues

To better understand the interaction between *S. sclerotiorum* and *C. sativa* at the cellular level, we conducted an anatomical survey of the infected *C. sativa* inflorescence tissue (Figure 3). We tracked fungal infection of the cola directly from the site of inoculation (Figure 3A). At 3 dpi, the inoculation site was clearly visible, as was the extension of fungal hyphae as *S. sclerotiorum* began to infect host floral tissue. At this timepoint, sectioning of reduced leaves proximal to the inoculation site revealed the presence of fungal hyphae along the surface of the epidermis as well as within epidermal cells, palisade mesophyll and general parenchymatic tissues, and phloem tissue of the vascular bundle (Figure 3B). Xylem tissues remained relatively untouched whereas the phloem showed extensive colonization by the fungus as compared to uninfected reduced leaves (Figure 3B-D). While the presence of fungal hyphae was found throughout the reduced leaf, minimal plant cell wall degradation was visible. By 7 dpi, the *C. sativa* reduced leaf showed severe degradation of all tissue layers apart from the xylem (Figures 3E). Although still structurally intact, *S. sclerotiorum* hyphae were visible throughout the xylem at this timepoint. The *C. sativa* stalked glandular trichomes of the inflorescence were also infected at this timepoint (Figure 3F).

In the floral stem of the plant, fungal hyphae were first seen to infect and degrade host phloem tissues. In areas of the stem nearest to the inoculated inflorescence, *S. sclerotiorum* was found to have extensively degraded phloem tissues of the main stem by 7 dpi (Figure 4A). Hyphae were also present within the xylem tracheids and pith; however, degradation of these tissues was limited (Figure 4B). Further from the site of inoculation, at the limit of hyphal travel within the stem, *S. sclerotiorum* was found only within the phloem (Figure 4C). Unlike areas

proximal to the inoculation site, host plant cell walls remained largely intact. Here, hyphae were not observed within the xylem nor the pith of the *C. sativa* stem (Figure 4D).

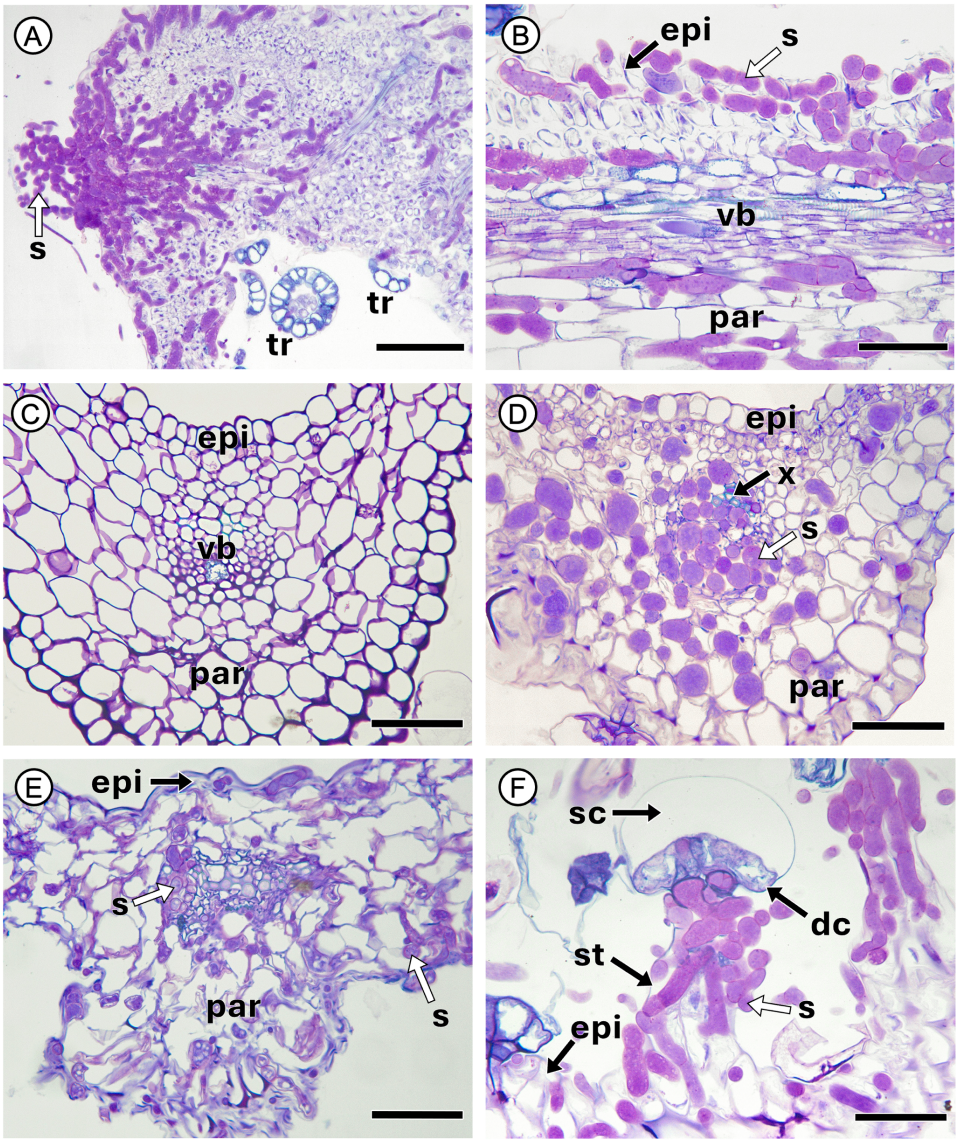

Figure 3. *S. sclerotiorum* infection of the *C. sativa* inflorescence and infection progression in reduced leaves. (A) Longitudinal section of the *S. sclerotiorum* inoculation site (s, white arrow) three days post inoculation. Trichomes (tr) are visible throughout the inflorescence. Scale bar = 100 µm. (B) Longitudinal section of the reduced leaf within the inflorescence. *S. sclerotiorum* hyphae (s, white arrow) found in epidermis (epi), parenchyma (par), and vascular bundle (vb) three days post inoculation. Scale bar = 50 µm. (C) Cross section of uninfected reduced leaf. Vascular bundle (vb), epidermal cells (epi) and parenchyma (par). Scale bar = 50 µm. (D) Cross section of reduced leaf three days post inoculation. *S. sclerotiorum* hyphae (white arrow) present throughout vascular bundle and parenchyma (par). Tracheary cells of the xylem (x) remain intact. Scale bar = 50 µm. (E) Cross section of reduced leaf seven days post inoculation. *S. sclerotiorum* hyphae (white arrow) present in epidermis (epi), parenchyma (par), and vascular bundle. Xylem (x) tracheary cells remain intact. Scale bar = 50 µm. (F) *S. sclerotiorum* infection of the stalk (st) and disk cells (dc) of a glandular trichome seven days post inoculation. Secretory cavity (sc) and cuticle are still intact. Scale bar = 50 µm.

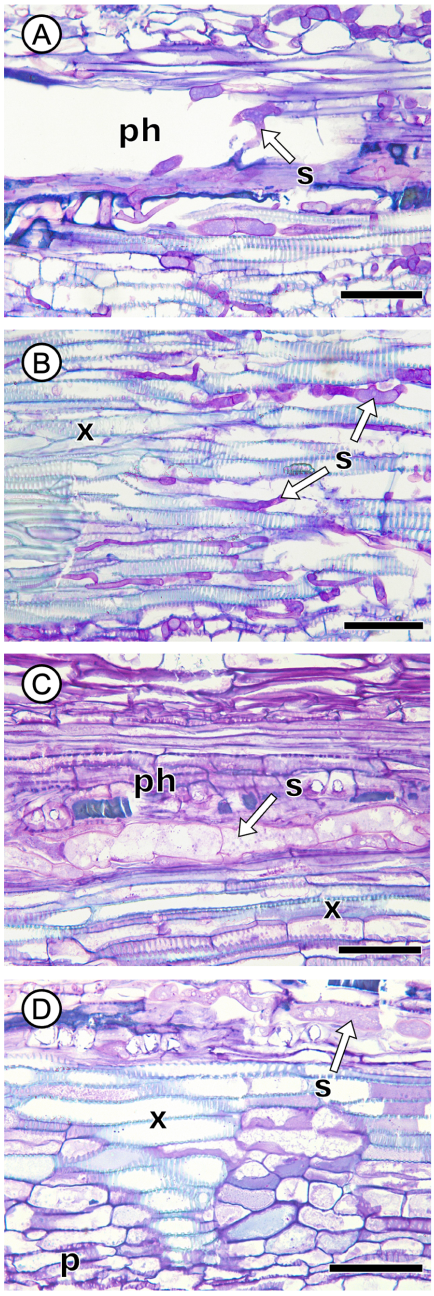

Figure 4. Longitudinal sections of the *C. sativa* inflorescence stem seven days post inoculation with *S. sclerotiorum.* (A) *C. sativa* stem vasculature proximal to the site of *S. sclerotiorum* inoculation. *S. sclerotiorum* hyphae (s, white arrow) present throughout the phloem (ph) which exhibits extensive degradation. Scale bar = 50 µm. (B) *C. sativa* stem vasculature proximal to the site of *S. sclerotiorum* inoculation. *S. sclerotiorum* hyphae (s, white arrow) within *C. sativa* xylem (x) tracheary cells seven days post inoculation. Scale bar = 50 µm. (C) *C. sativa* stem vasculature distal to the site of *S. sclerotiorum* inoculation. *S. sclerotiorum* hyphae present in phloem (ph) and absent in xylem (x). Phloem remains intact. Scale bar = 50 µm. (D) *C. sativa* stem vasculature distal to the site of *S. sclerotiorum* inoculation. *S. sclerotiorum* hyphae present in phloem (ph), while no hyphae are present in xylem (x) or pith (p). Scale bar = 50 µm.

Differential gene expression analysis reveals the induction of *C. sativa* defense responses and altered terpenoid production at the mRNA level by *S. sclerotiorum*

Next, we carried out differential gene expression analysis to better understand how *C. sativa* responds to *S. sclerotiorum* at the mRNA level (Figure 5). The largest number of up-regulated differentially expressed genes in *C. sativa* were found at the intersection of 3-, 5- and 7 dpi, and of 3- and 5 dpi, with 2937 and 1855 genes, respectively (Figure 5A). Specific to each timepoint, 4 genes were upregulated at 1 dpi, 393 genes at 3 dpi, 861 genes at 5 dpi, and 850 genes at 7 dpi. To better understand the biological and molecular processes associated with these gene sets, we conducted a GO enrichment analysis (Figure 5B). Enriched at all timepoints were GO terms associated with terpene biosynthesis (terpene synthase activity $P = 4.13x10^{-9}$ and diterpenoid biosynthetic process ($P = 4.08x10^{-8}$), plant stress responses (abscisic acid binding $P = 7.84x10^{-5}$, response to oxidative stress P = 0.0001), plant defense (P = 0.001), and chitinase activity (P = 0.0005). Specific to 3- and 5 dpi, we observed enrichment of GO terms associated with protein synthesis/transport (translation $P = 1.73x10^{-63}$ and endoplasmic reticulum to Golgi vesicle-mediated transport $P = 4.81x10^{-11}$). Shared between 5- and 7 dpi, were GO terms involved in hormone signalling (regulation of jasmonic acid signalling $P = 9.98x10^{-7}$ and regulation of SA biosynthesis P = 0.0021), response to wounding ($P = 6.17x10^{-5}$), and calcium/calmodulin signalling (P = 0.0025 and P = 0.0099). More generally, shared between 3-, 5-, and 7 dpi were terms pertaining to oxidative stress responses (glutathione metabolic process $P = 1.42x10^{-12}$ and hypersensitive response P = 0.0011), ethylene signalling ($P = 1.34x10^{-6}$), and protein kinase and protein ser/thr kinase activity ($P = 7.99x10^{-6}$ and 0.00046).

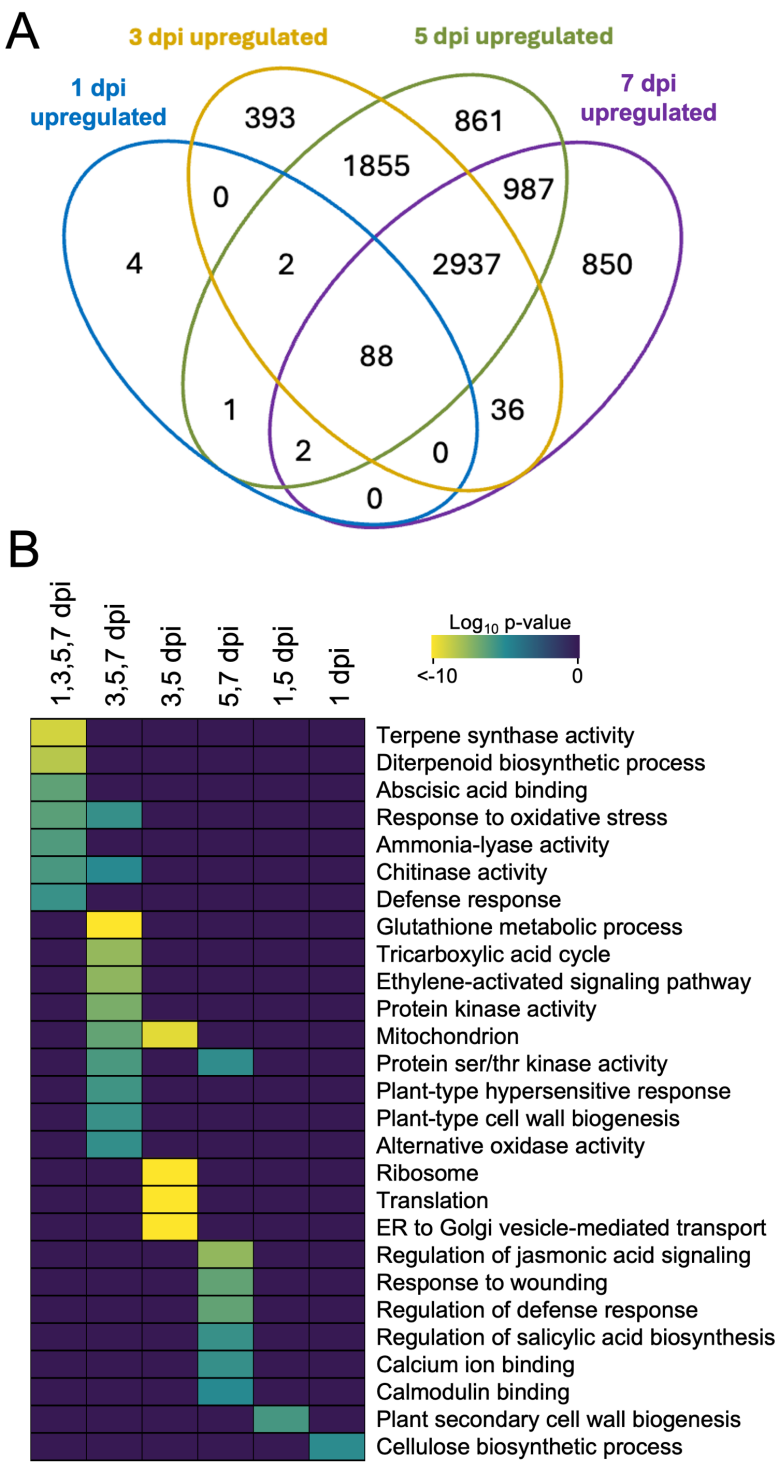

Figure 5. Upregulated differential gene expression of *C. sativa* infected with *S. sclerotiorum* over a seven-day infection period. (A) Venn diagram of significantly upregulated differentially expressed gene sets (FDR<0.05) in response to infection. (B) Heatmap of significantly enriched GO terms (FDR <0.01) resulting from timepoint-specific and shared subsets. A brighter yellow colour indicates greater statistical significance. dpi = days post inoculation.

In response to infection, we uncovered genes encoding chitinases and endochitinases to be upregulated in *C. sativa* (Figure 6). Those with highest fold changes in response to infection at 5 dpi included *ENDOCHINTINASE 2* (*LOC115705823*; 1982-fold) and *ENDOCHITINASE-LIKE* (*LOC133037227*; 1074-fold). Also seen to be highly upregulated at 5 dpi were genes involved the plant SAR response, including *PATHOGENESIS RELATED* (*PR*) genes. These genes included *THAUMATIN-LIKE PROTEIN 1B* (*PR5; LOC115710654*; 3487-fold), *PATHOGENESIS-RELATED PROTEIN STH-2* (*PR10a; LOC115722015;* 917-fold) and *MAJOR ALLERGEN PRU AV 1* (*PR10; LOC115722031*; 899-fold). Additionally, we observed the induction of genes involved in JA/ET hormone signalling. *JASMONATE-ZIM DOMAIN* (*JAZ*) protein genes *JAZ5* and *JAZ8* in addition to *ETHYLENE RESPONSIVE FACTORs* (*ERF*) *ERF096* and *ERF098* were also significantly differentially expressed. Furthermore, we uncovered notable upregulation of numerous receptor-like kinase (RLK) genes that included *WALL ASSOCIATED RECEPTOR KINASE 2* (*WAK2; LOC115708008*) and *WALL ASSOCIATED RECEPTOR KINASE-LIKE 1* (*WAKL1; LOC115696698*) which both exhibited a 500-fold increase in expression, in addition to various other serine/threonine RLKs that include *G-TYPE LECTIN S-RECEPTOR-LIKE SERINE/THREONINE-PROTEIN KINASE 3* (*LECRK3; LOC113032648*) and *LECRK4* (*LOC115721224*). Finally, a number of peroxidases in *C. sativa* were also found to be highly upregulated in response to *S. sclerotiorum*. These peroxidases included *PEROXIDASE 57* (*PER57; LOC115722259*), *CATIONIC PEROXIDASE 1* (*LOC115720664*), *LIGNIN-FORMING ANIONIC PEROXIDASE* (*LOC115723064*), and *PEROXIDASE 5-LIKE* (*LOC115723295*) with fold changes at 5 dpi of 9710, 2868, 2375, and 1470, respectively.

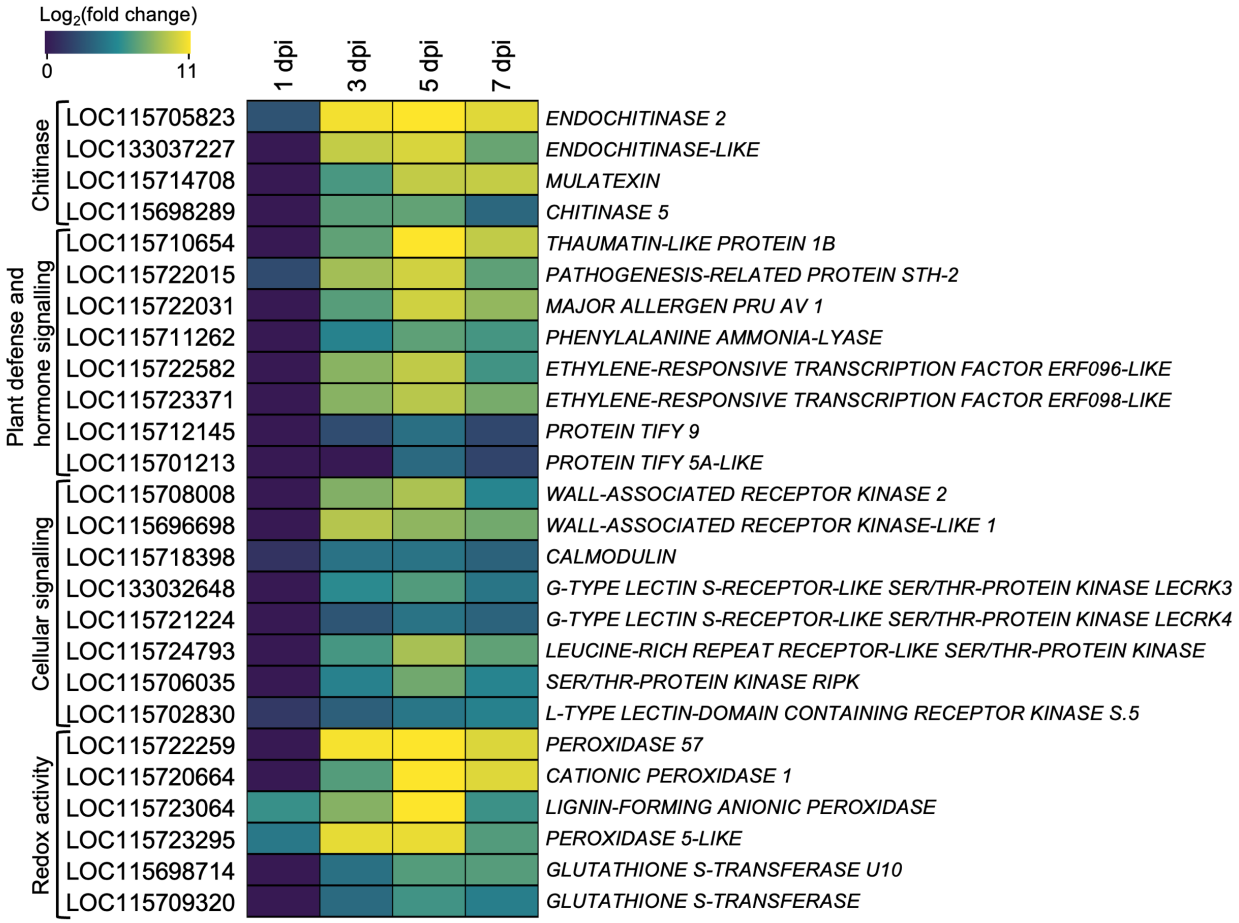

Figure 6. Heatmap of significantly differentially expressed *C. sativa* genes (FDR<0.05) belonging to enriched GO terms following inoculation with *S. sclerotiorum*. Brighter yellow colour indicates a greater fold change in expression compared to uninfected plants. dpi = days post inoculation.

We were next interested in understanding the genes and biological processes that were downregulated in *C. sativa* in response to infection with *S. sclerotiorum* (Figure S4). The largest number of down-regulated genes were shared between 3-, 5- and 7 dpi (2866 genes; Figure S4A). Large numbers of shared DEGs were also observed between 3- and 5 dpi (1458 genes) and 5- and 7 dpi (1179 genes). Specific to each timepoint, we identified 850 DEGs at 7 dpi, 1540 DEGs at 5 dpi, 512 at 3 dpi, and interestingly, 0 at 1 dpi. We then carried out a GO term enrichment to better understand the biological processes and molecular functions associated with these gene sets (Figure S4B). GO terms associated with photosynthesis ($P = 1.64x10^{-8}$), cellular development ($P = 2.09x10^{-5}$) and terpene synthesis (diterpenoid biosynthetic process P = 0.0002, terpene synthase activity P = 0.0008) were shared between 3-, 5-, and 7 dpi. Abscisic acid biosynthesis (P = 0.005) was enriched in gene sets shared between 3- and 5- dpi while biological processes associated with hormone activity like jasmonic acid biosynthesis (P = 0.0003) and cytokinin signalling (P = 0.0087) were specific to gene sets at 3 dpi.

While terpene/diterpenoid biosynthesis GO terms were enriched in both up and downregulated gene sets, the specific genes involved in either GO term were unique (Figure 7). Upregulated in response to *S. sclerotiorum* infection were *C. sativa* terpene synthases that included *MONOTERPENE SYNTHASE MTS1* (*LOC133031472, LOC115723097, LOC133030985, LOC115723096, LOC115723095*) and *(-)-GERMACRENE D SYNTHASE-LIKE* (*LOC115707304*). Both genes were highly upregulated with fold changes as high as 6361 at 7dpi (*LOC13303985*) and 6400 at 5dpi (*LOC115707304*). Conversely, genes downregulated in response to infection included *ALPHA-HUMULENE SYNTHASE* and -*SYNTHASE-LIKE* (*LOC115695864, LOC115695866, LOC115725506* and *LOC133038934, LOC133039417,*

LOC115715212), *(E-E)-GERANYLLINALOOL SYNTHASE* (*LOC115696242*), *(-)-LIMONENE SYNTHASE* (*LOC115716064, LOC115716066, LOC133037760*) and *MYRCENE SYNTHASE* (*LOC115716405, LOC133029092, LOC133037756*). Some of the most downregulated genes included *(E-E)-GERANYLLINALOOL SYNTHASE* (14.8-fold compared to uninfected plants at 7 dpi) and *ALPHA-HUMULENE SYNTHASE* (*LOC115725506;* 14.6-fold compared to uninfected plants at 5 dpi).

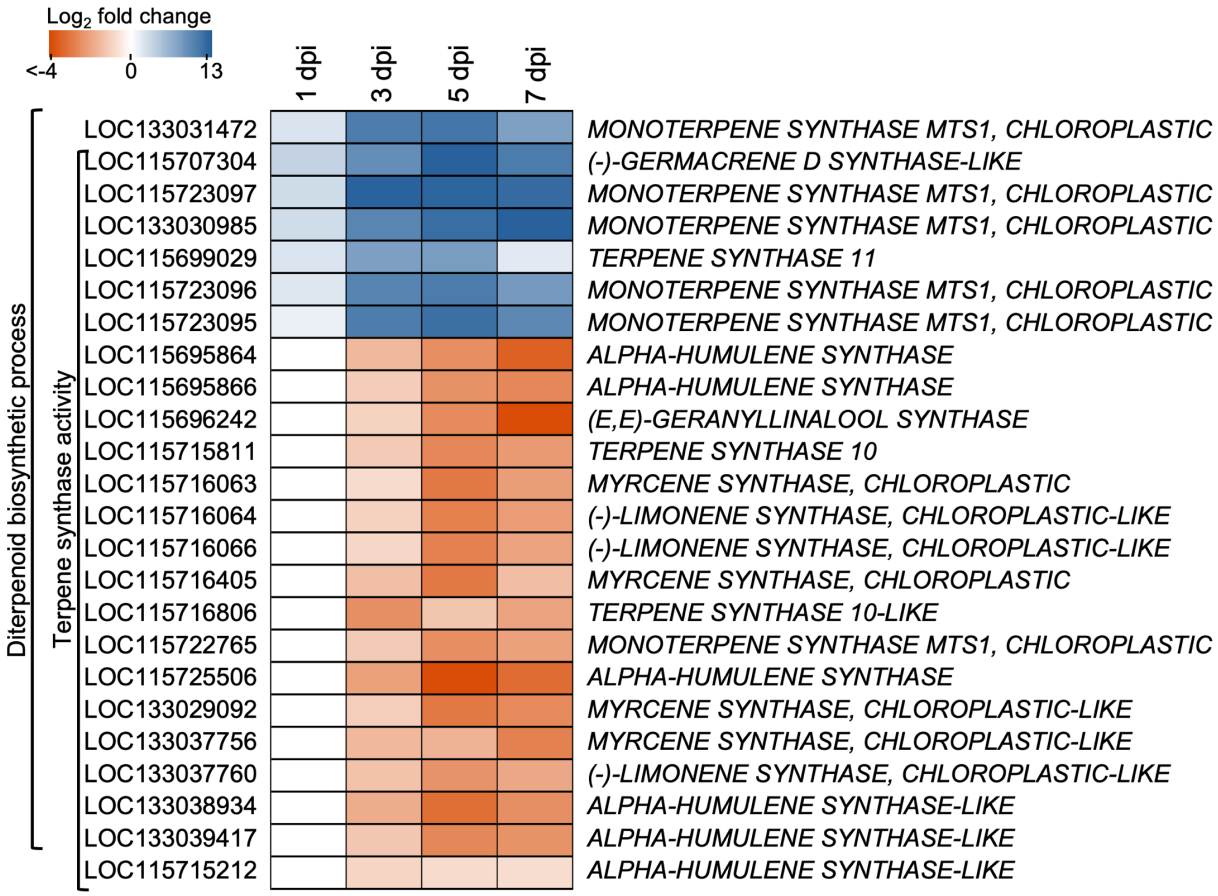

Figure 7. Heatmap of significantly up- and downregulated *C. sativa* genes of the diterpenoid biosynthetic process and terpene synthase activity in response to *S. sclerotiorum* (FDR <0.05). Colour corresponds to log_2fold change, where a saturated orange colour corresponds to a greater log_2fold change downregulation, and a saturated blue colour corresponds to a greater log_2fold change upregulation. dpi = days post inoculation.

Differential gene expression analysis of *S. sclerotiorum* infecting *C. sativa* identified biological processes associated with carbohydrate metabolic activity and REDOX processing

To investigate changes in *S. sclerotiorum* gene activity during *C. sativa* infection, we carried out differential gene expression and gene ontology term enrichment analysis (Figure 8). Differential expression analysis revealed a high degree of shared differentially expressed genes at all sample timepoints (770 upregulated DEGs; Figure 8A). Further, we observed the specific upregulation of 308 DEGs at 1 dpi, 95 at 3 dpi, 198 at 5 dpi, and 877 at 7 dpi. GO terms associated with host plant cell wall breakdown and carbohydrate metabolism (carbohydrate metabolic process $P = 6.06x10^{-10}$, cellulose binding $P = 7.54x10^{-8}$, xylan catabolic process $P = 8.18x10^{-5}$, polygalacturonase activity P = 0.001) in addition to protein serine/threonine kinase activity (P = 0.0005) were shared across all time points. GO terms associated with carbohydrate and cell wall breakdown, in addition to fungal growth and development within the host (P = 0.0007) were enriched in gene sets shared between 3-, 5-, and 7- dpi. REDOX processes and homeostasis were enriched in both the 3-, 5-, 7 dpi shared group, and the 3- 7 dpi shared group with P = 0.001 and P = 0.006, respectively (Figure 8B).

Differential gene expression analysis of downregulated genes identified large numbers of shared DEGs shared between all sampled time points (610 genes) and shared between 3-, 5- and 7 dpi (710 genes; Figure S5A). Gene ontology terms enriched across all sampled timepoints identified enriched GO terms associated with translation and protein folding (ribosome P = 0.0005, translation $P = 3.47x10^{-5}$, unfolded protein binding P = 0.0007, and protein folding P =

0.004) in addition to mitochondrial activity (mitochondrion P = 0.002, tricarboxylic acid cycle P = 0.0001) (Figure S5B).

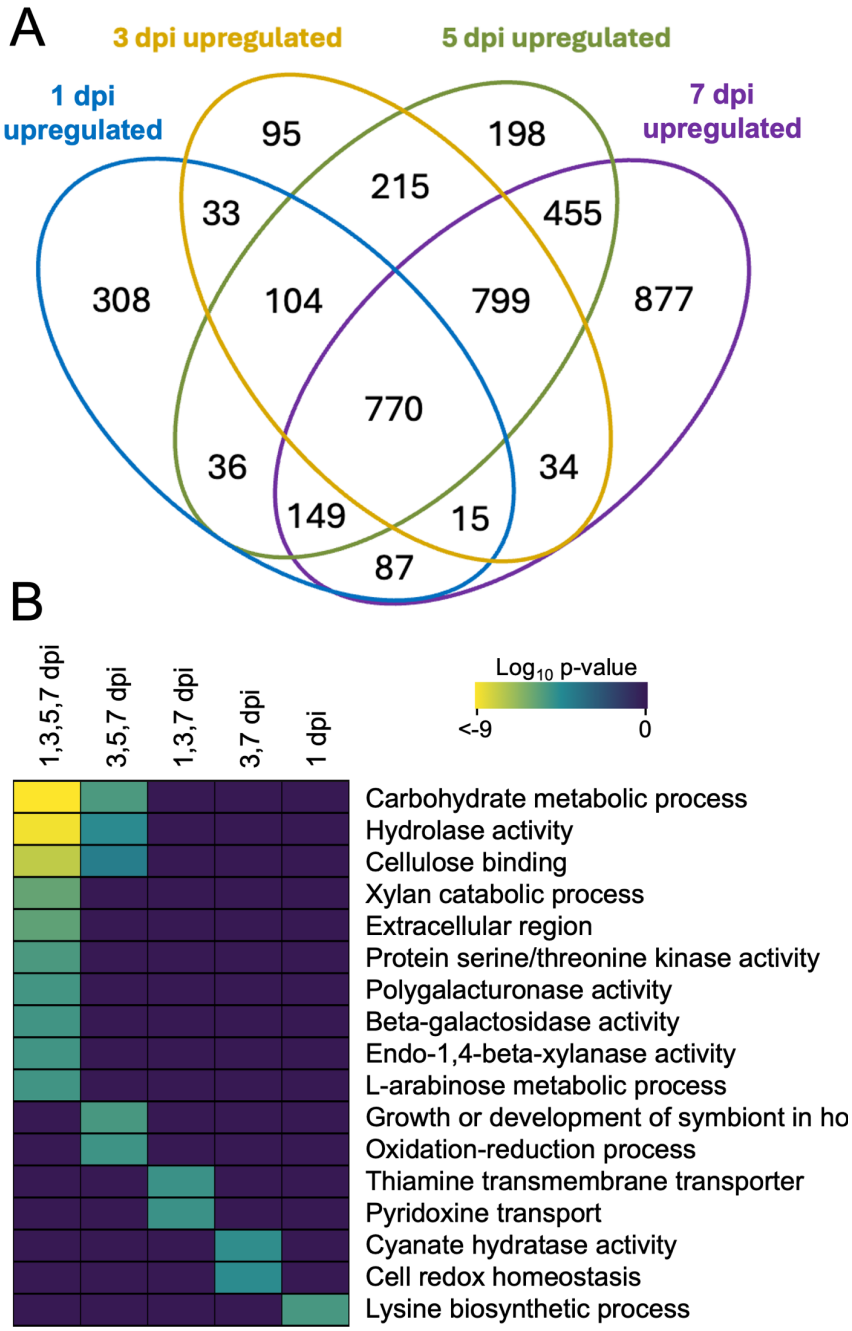

Figure 8. Upregulated differential gene expression of *S. sclerotiorum* infecting *C. sativa* across a seven-day infection period. (A) Venn diagram of significantly upregulated differentially expressed gene sets (FDR<0.05) in response to infection. (B) Heatmap of significantly enriched GO terms (FDR <0.01) resulting from timepoint-specific and shared subsets. A brighter yellow colour indicates greater statistical significance. Differentially expressed genes were compared to in vitro grown *S. sclerotiorum*. dpi = days post inoculation.

Supplemental figures

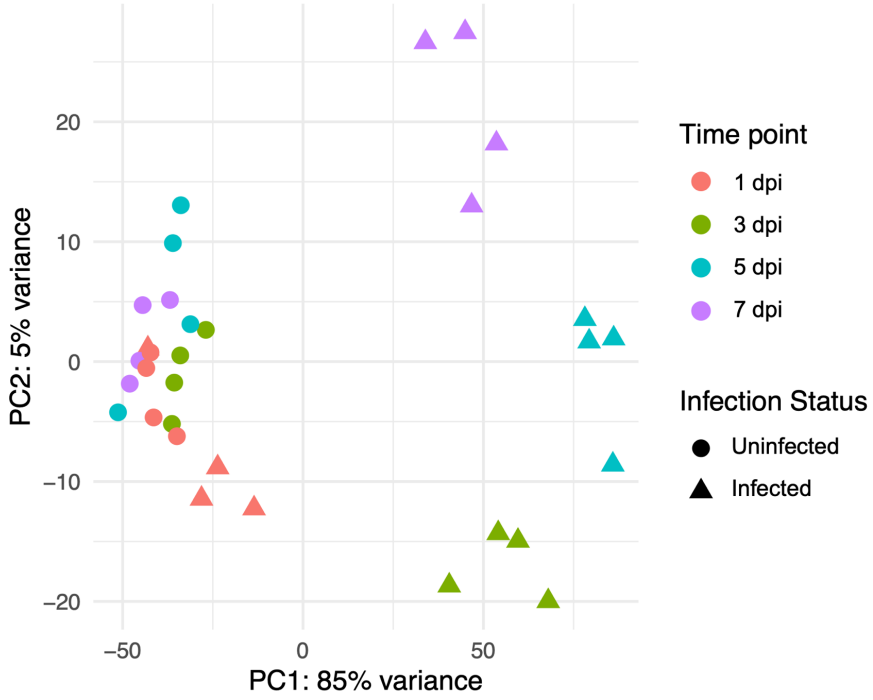

Figure S1. Principal component analysis (PCA) of *C. sativa* in the presence and absence of *S. sclerotiorum* across a seven-day infection period. Circles correspond to uninfected tissues, while triangles correspond to infected tissues. Colour corresponds to timepoint. PCA generated considering the top 1000 most variable genes. dpi = days post inoculation.

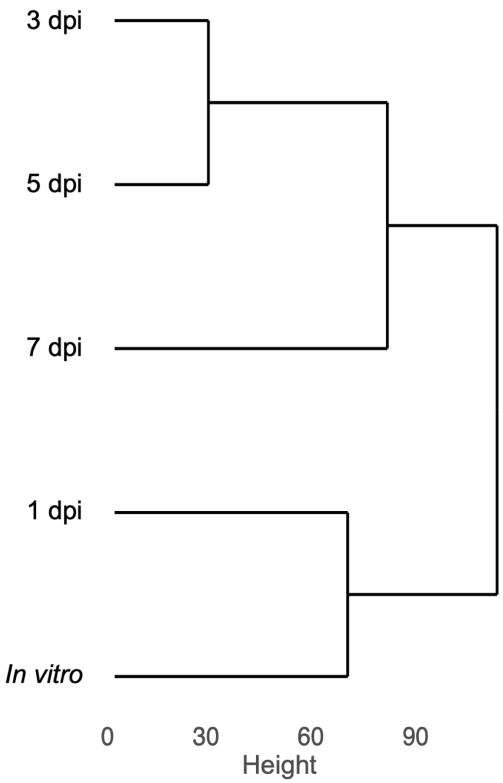

Figure S2. Hierarchical clustering of the top 1000 most variable genes of *S. sclerotiorum* grown *in vitro* or *in planta* during infection of *C. sativa*. Height corresponds to distance between clusters as computed by Euclidian distance. dpi = days post inoculation.

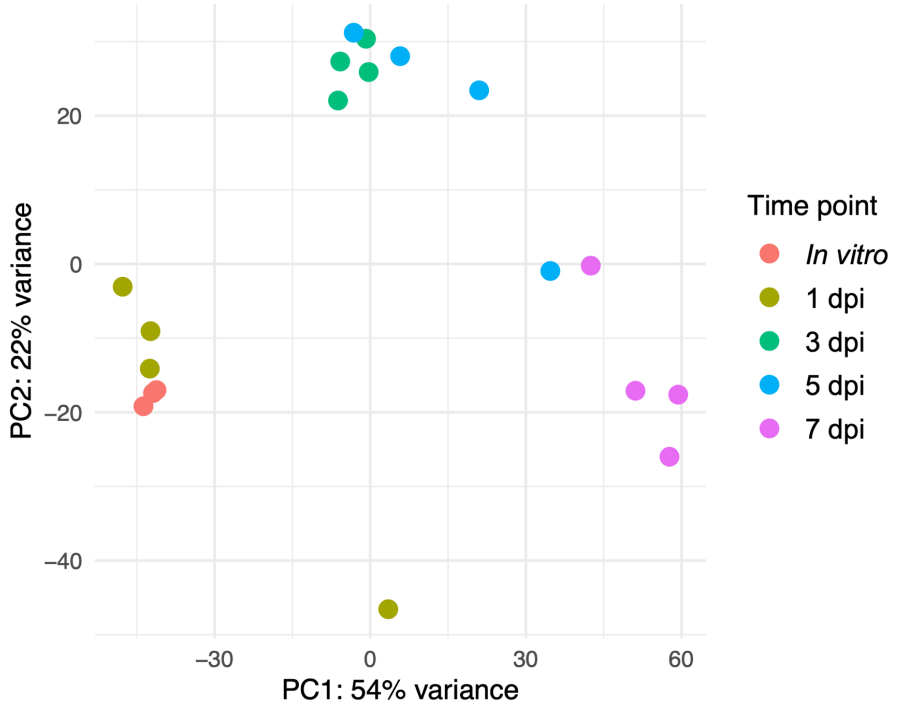

Figure S3. Principal component analysis (PCA) of *S. sclerotiorum* grown *in vitro* or *in planta* during a seven-day infection of *C. sativa*. Colour corresponds to timepoint, while red corresponds to *in vitro* grown *S. sclerotiorum*. PCA generated considering the top 500 most variable genes. dpi = days post inoculation.

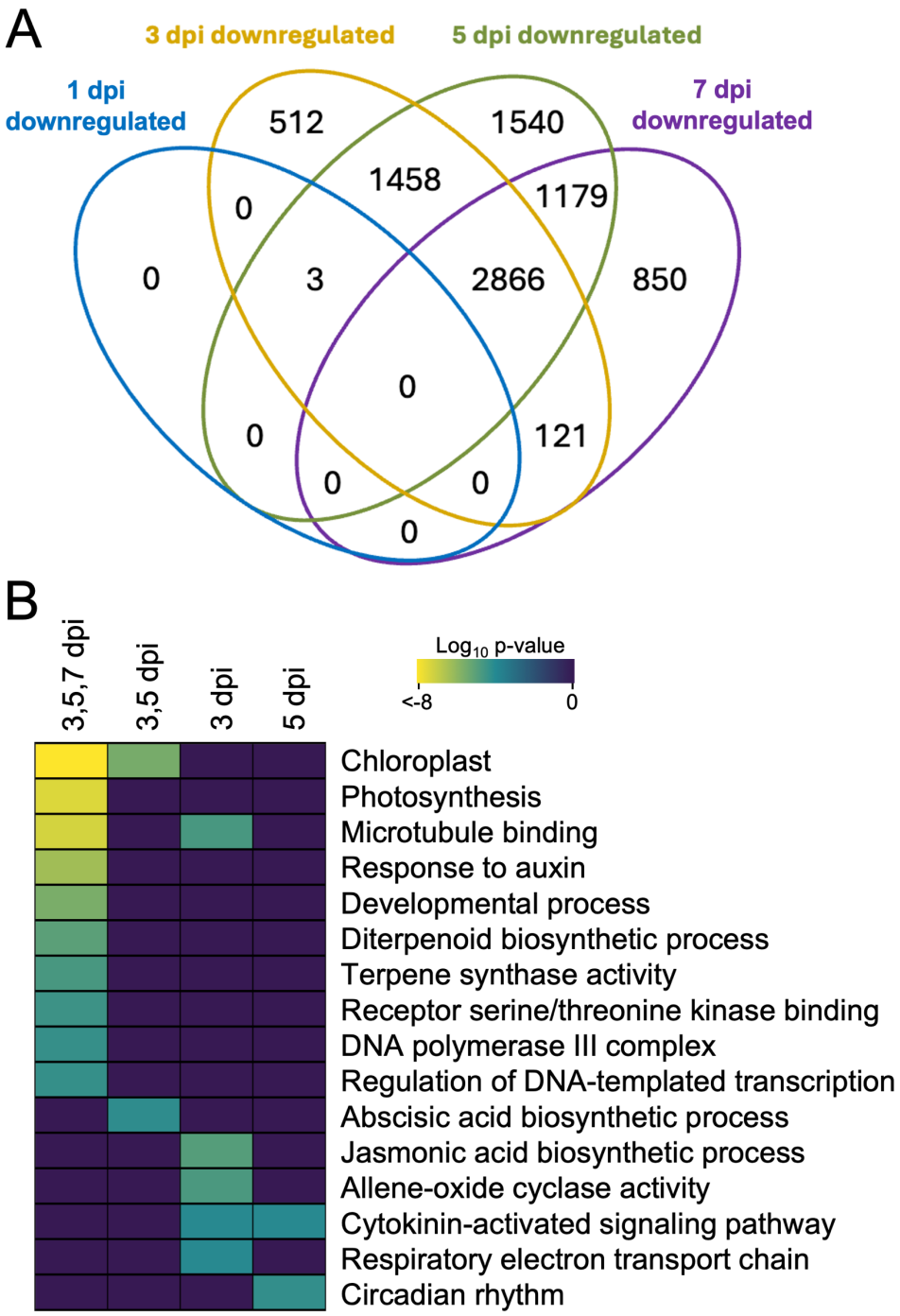

Figure S4. Differential gene expression analysis of down-regulated genes in *C. sativa* infected with *S. sclerotiorum* across a seven-day infection period. (A) Venn diagram of significantly downregulated differentially expressed gene sets (FDR<0.05) in response to infection. (B) Heatmap of significantly enriched GO terms (FDR <0.01) resulting from timepoint-specific and shared subsets. A brighter yellow colour indicates greater statistical significance. dpi = days post inoculation.

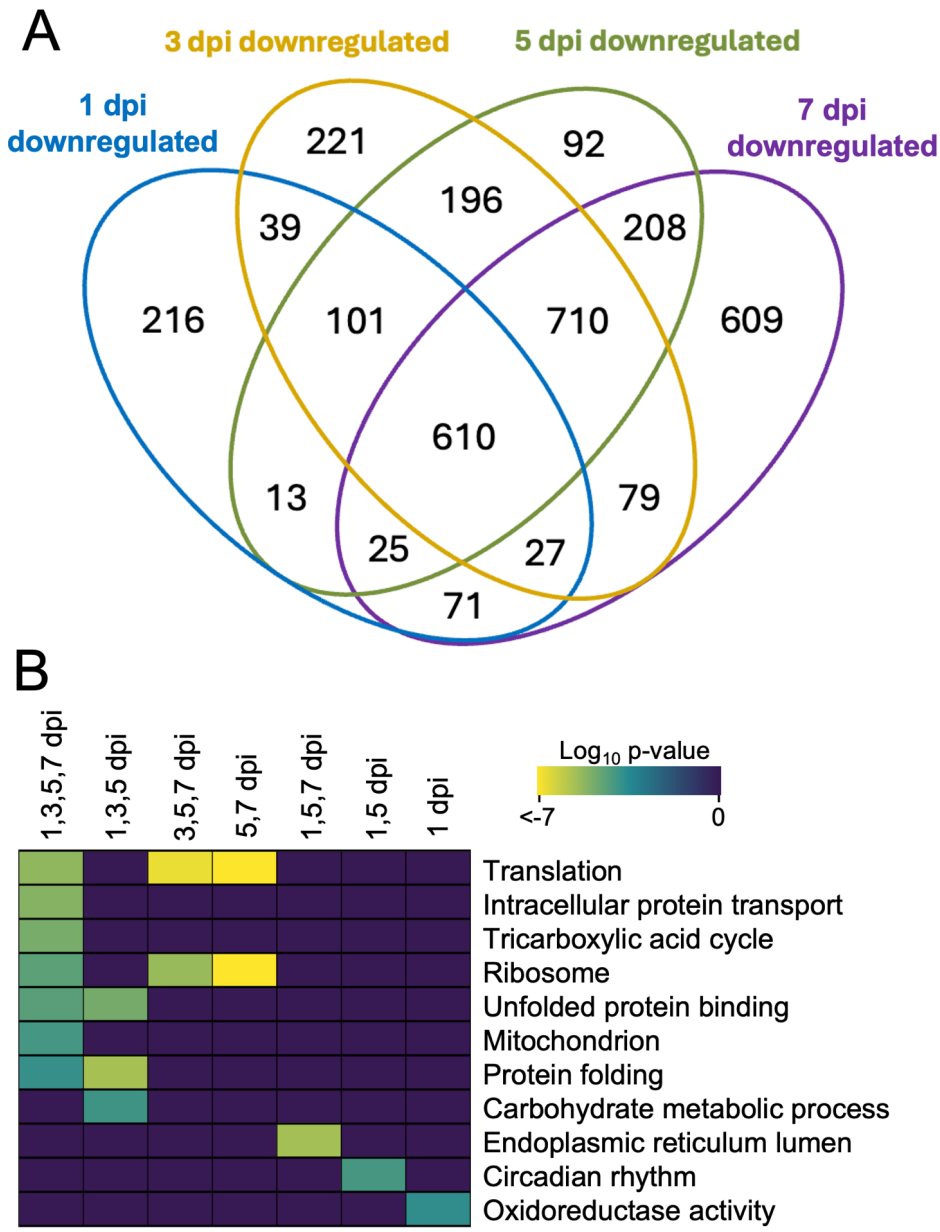

Figure S5. Differential gene expression analysis of significantly downregulated gene sets of *S. sclerotiorum* infection of *C. sativa* across a seven-day infection period. (A) Venn diagram of significantly downregulated differentially expressed gene sets (FDR<0.05) in response to infection. (B) Heatmap of significantly enriched GO terms (FDR <0.01) resulting from timepoint-specific and shared subsets. A brighter yellow colour indicates greater statistical significance. dpi = days post inoculation.

CHAPTER FOUR: Discussion

As a result of legal constraints in effect around the world, *C. sativa* remains greatly understudied compared to other crop species. Even in Canada, where non-medical *Cannabis* sale was legalized in 2018 (Government of Canada, 2018), there exist strict government regulations that limit "drug-type" *C. sativa* cultivation and research only to those with appropriate permits (Punja, 2021). As such, there is currently a lack of published literature focused on exploring the interactions between *C. sativa* and devastating fungal pathogens such as *S. sclerotiorum*, notably at the transcriptomic level. This study serves as the first description of the *Cannabis*-*Sclerotinia* pathosystem at the mRNA level where we show the rapid initiation of *S. sclerotiorum* infection in the *C. sativa* inflorescence. Within a week of infection, severe disease symptoms were widespread in the plant. Global gene activity underpinning this interaction revealed *C. sativa* responds to infection through the elicitation of lignin deposition, REDOX buffering and generalized plant defense/immune hormone signalling cascades at the mRNA level. Anatomical investigation at the site of inoculation showed the rapid colonization and degradation of host plant tissues by *S. sclerotiorum* starting in the epidermis and mesophyll before targeting the vascular system of the plant. While this work focused on the infection of the *C. sativa* inflorescence; *S. sclerotiorum* has also been documented to cause extensive damage to the *C. sativa* stem and crown in infection reports from both field- and greenhouse-grown plants (Bains et al., 2000; Garfinkel, 2021; Yang et al., 2023).

Known now as both a stem and bud rot pathogen, *S. sclerotiorum* is regarded as an emerging fungal pathogen of *C. sativa* (Punja & Ni, 2021). To date, there remains to be a study that describes the detailed transcriptomic response of *C. sativa* to infection with any necrotrophic

fungal pathogen. Currently, few transcriptome-level studies of *C. sativa* exist, with those published focussing on sex determination and plasticity (Adal et al., 2021; Monthony et al., 2024; Prentout et al., 2020), specialized secondary metabolite production (Braich et al., 2019; Yeo et al., 2022), or response to abiotic stresses such as salinity, drought, and heavy metals (Huang et al., 2019; Liu et al., 2016; J. Zhang et al., 2021).

C. sativa responds to *S. sclerotiorum* through rapid and profound changes in gene expression profiles across the seven-day infection period. Detection of plant pathogens ties together the concepts of PTI and ETI, where unique molecular responses are initiated as a result of the recognition of pathogenic elicitors, PAMPs or damage associated molecular patterns (DAMPs) (Dodds et al., 2024; Pruitt et al., 2021). In response to *S. sclerotiorum* infection, we uncovered the upregulation of genes whose products are involved in pathogen perception and early defense responses such as ser/thr RLKs, NLRs, wall associated kinases (WAK) and WAK-like proteins (WAKL) (Dodds et al., 2024; Kohorn & Kohorn, 2012). Specific to our dataset, we saw notable upregulation of genes *WAK2* (*LOC115708008*) and *WAKL1* (*LOC115696698*) whose expression increased 500% at days 3 and 5 post infection. WAKs and WAKLs have long been known to play a role in the plant defense response to pathogens (C. Stephens et al., 2022; Yan et al., 2023). Considered as members of one of the fifteen subfamilies of RLKs found in plants, WAKs bind pectin and oligosaccharides (fragmented pectin) which act as DAMPs during biotic stress responses (Harvey et al., 2024). Expression of WAKs, including *WAK1* in *Arabidopsis thaliana*, have been shown to be upregulated both in response to SA accumulation and in response to wounding (He et al., 1998). WAKs/WAKLs have previously been shown to confer resistance against both hemibiotrophic and necrotrophic fungal pathogens through various

mechanisms that include cell wall restructuring and pathogen- or host-derived elicitor detection (Stephens et al., 2022). Additional studies conducted in transgenic *A. thaliana* have reported that ectopic expression of *WAK1* resulted in increased resistance to *B. cinerea* (Brutus et al., 2010), while *WAKL10* knockout resulted in increased susceptibility to *Pseudomonas syringae* (Bot et al., 2019; Stephens et al., 2022). In addition to *A. thaliana,* immunity-related WAKs/WAKLs have been documented in both monocotyledonous and dicotyledonous crop species in response to pathogen attack. These species include *Triticum aestivum* (wheat), *Oryza sativa* (rice), *Hordeum vulgare* (barley), *Zea mays* (maize), *Sesamum indicum* (sesame), *Solanum lycopersicum* (tomato), *Gossypium hirsutum* (cotton), and *Brassica napus* (canola) thus suggesting WAKs/WAKLs as an evolutionarily conserved feature of the plant defense response against fungal necrotrophs (Stephens et al., 2022; Wu et al., 2016; Yan et al., 2023). Notable upregulation of *WAK2* and *WAKL1* expression midway through the seven-day infection period begs the questions of whether earlier induction of these genes in *C. sativa* would result in greater fungal resistance, leaving room for further study.

The plant's cell wall is the first line of defense that serves as a barrier to restrict attacking pathogens. Fungal necrotrophic pathogens make use of CWDEs to impair cell wall integrity and ultimately degrade host plant tissues (Bellincampi et al., 2014). Despite the presence of *S. sclerotiorum* throughout the epidermis, mesophyll and vasculature of the *C. sativa* leaf at 3 dpi, cell wall degradation at this timepoint was not yet observed. In comparison, previous studies have detailed extensive cellular degradation resulting from *S. sclerotiorum* infection as early as 2 dpi in leaves of *B. napus* (Girard et al., 2017) and *A. thaliana* (Walker et al., 2023), and 3 dpi in *Glycine max* (soybean; Davidson et al., 2016). Our data show that progression of *S. sclerotiorum*

into *C. sativa* leaf tissues progressed more slowly, however it should be noted that this delay could be the result of the complex three-dimensional structure of the cola, versus the direct inoculation of the leaf as was used in the above studies. Work carried out by Wytinck et al. (2022) in the *B. napus* stem showed similar findings where *S. sclerotiorum* infection resulted in extensive colonization and degradation of the host epidermis, cortex, and phloem, while xylem tissues remained largely intact. These results suggest a shared infection strategy by *S. sclerotiorum* across diverse plant species, despite the structural and complex metabolic differences *C. sativa* exhibits compared to other crop plant species.

Our gene ontology analysis revealed the enrichment of cell wall degrading activities in *S. sclerotiorum* as infection was initiated in *C. sativa*. Hydrolase activity, xylan catabolic process, polygalacturonase activity, beta-galactosidase activity, and 1,4-beta-xylanase activity were found across all infection time points. Production of CWDEs by *S. sclerotiorum* facilitates tissue penetration and maceration, through cell wall weakening characteristic of necrotrophic fungal infection (Bolton et al., 2006). Polygalacturonases (PGs) are a class of fungal pectinases that target unesterified pectate polymers of the middle lamella and primary cell wall of the host plant (Bolton et al., 2006). As plant cell walls are weakened and degraded by PGs, the secreted oligogalacturonides have been shown to elicit ROS burst, including H_2O_2 and O_2^-, as the plant attempts to restrict pathogen attack (Bolton et al., 2006; Wojtaszek, 1997). While these ROS play important roles as early defense signalling molecules, when present in higher concentrations they also cause oxidative damage to host molecular machinery and can result in cell death (Girard et al., 2017). ROS production to develop localized cell death occurring as a result of pathogen infection is termed as the plant hypersensitive response (HR), and is regarded as one of the most

important factors in impeding the growth of biotrophic pathogens (Govrin & Levine, 2000). Although the localized cell death associated with the HR is generally effective against biotrophic pathogens, necrotrophic pathogen virulence, including that of *S. sclerotiorum* and *B. cinerea*, has been suggested to be strengthened as a result of HR elicitation (Hegedus & Rimmer, 2005; Rossi et al., 2017). Studies in *Nicotiana tabacum* (tobacco) and *A. thaliana* have also revealed that plants unable to initiate the HR demonstrated increased resistance to *S. sclerotiorum* (Dickman et al., 2001; Thomma et al., 2001). While we uncovered rapid upregulation of *S. sclerotiorum* PG activity that continued throughout the seven-day infection period, the *C. sativa* HR was not induced until 3 dpi, likely revealing one facet of the *S. sclerotiorum* coordinated and timed control of host ROS activation to favour fungal proliferation in host tissues.

Similarly, the major *S. sclerotiorum* pathogenicity factor OA, has also been previously found to manipulate host ROS production such that it initially suppresses ROS signalling, before eliciting ROS production, leading to cell death (Cessna et al., 2000; Girard et al., 2017). Recent studies have challenged the classical view of the *S. sclerotiorum* necrotrophic lifestyle, suggesting the possibility of a brief biotrophic phase early in the infection process. These studies suggest that *S. sclerotiorum* is capable of suppressing SA-mediated SAR early in infection, and thus the HR, before the true necrotrophic portion of the lifestyle occurs in which initiation of ROS production leads to localized cell death and subsequent widespread infection (Kabbage et al., 2015; Seifbarghi et al., 2017). Previous studies have deemed OA to be an essential *S. sclerotiorum* pathogenicity factor as various plant species have been capable of mounting an early defense response, through the deployment of ROS burst and callose deposition, against OA-deficient mutant strains of *S. sclerotiorum* (Cessna et al., 2000; Kabbage et al., 2015;

Williams et al., 2011). Our results support the initial suppression of SA-dependent SAR as *PHENYLALANINE AMMONIA-LYASE* (*PAL*), a major enzyme involved in SA biosynthesis, was not upregulated until 3 dpi, with highest upregulation occurring two days later, at 5 dpi. This aligns with previous findings in *B. cinerea*-infected *C. sativa* leaf tissue where *PAL* activity was upregulated at much higher levels later in infection (7 dpi) than earlier in infection (2 dpi) (Balthazar et al., 2020). Similarly, we found *GLUTATHIONE S-TRANSFERASE U10* (*LOC115698714*) and *GLUTATHIONE S-TRANSFERASE* (*LOC115709320*) were not upregulated until 3 dpi. Glutathione transferases are cellular protectant enzymes involved in REDOX homeostasis and ROS detoxification that are rapidly induced by H_2O_2 (Lamb & Dixon, 1997). Previous work in *B. napus* revealed plants partially resistant to *S. sclerotiorum* demonstrated increased REDOX buffering capacity as early as 1 dpi (Girard et al., 2017). These results suggest that a more rapid induction of REDOX buffering by *C. sativa* may result in an increased resistance or tolerant phenotype. Furthermore, we uncovered upregulation of ERF transcription factors *ERF98-like* (*LOC115723371*) and *-96-like* (*LOC115722582*) as early as 3 dpi, and with highest expression levels at 5 dpi. Work by Girard *et al.* (2017) in the *B. napus – S. sclerotiorum* pathosystem also uncovered upregulation *ERF98* in response to *S. sclerotiorum* infection, noting that expression was higher in a *S. sclerotiorum*-resistant *B. napus* cultivar than in a susceptible control. *ERF98* is an ET- and H_2O_2-induced transcription factor that is known to upregulate the biosynthesis of ascorbic acid, and was previously proposed as a regulator of REDOX-related defense responses in the *B. napus*-*S. sclerotiorum* pathosystem (Girard et al., 2017; Wang et al., 2013). Through resolving the timing of ROS signalling at the host-pathogen interface, our data not only support the hypothesized initial biotrophic phase where *S.*

sclerotiorum suppresses SA-mediated SAR but also support *ERF98* as a regulator of REDOX-related defense responses in *C. sativa.*

In addition to ROS accumulation, *S. sclerotiorum* infection has previously been found to initiate lignin biosynthesis within the host plant (Calla et al., 2014). Lignins are biopolymers important for plant cell wall structural support, and have previously been reported to be deposited in *Brassica* species in response to *S. sclerotiorum* infection (Uloth et al., 2016). They are synthesized through a H_2O_2-dependent, PAL-catalyzed reaction to produce monolignols which then undergo peroxidase-mediated oxidative polymerization to produce lignin (Calla et al., 2014). Specific to our study, we found that in response to *S. sclerotiorum* infection, *C. sativa* highly upregulated *PAL* (*LOC115711262*) in addition to various class III peroxidases that include *PEROXIDASE 57* (*LOC115722259*), *CATIONIC PEROXIDASE 1* (*LOC115720664*), *LIGNIN-FORMING ANIONIC PEROXIDASE* (*LOC115723064*), and *PEROXIDASE 5-LIKE* (*LOC115723295*). Belonging to the PR-9 subfamily of PR proteins, class III plant peroxidase gene expression has previously been found to increase in plants challenged with fungi, in addition to bacteria, viruses and viroids (Almagro et al., 2009; Sasaki et al., 2004; van Loon et al., 2006). Plant peroxidases are also capable of creating physical barriers to limit pathogen invasion in response to stimuli such as wounding, pathogen presence, or hormone accumulation (Almagro et al., 2009). Both SA and JA have independently been found to positively regulate peroxidase gene expression, however the effects of SA-JA hormone crosstalk in peroxidase regulation has yet to be described (Almagro et al., 2009). The upregulation of peroxidase activity uncovered in this study serves as the first description of genes involved in H_2O_2-dependent lignin deposition by *C. sativa* to restrict further incursion of *S. sclerotiorum*.

Hormone crosstalk between SA and JA pathways has long been documented, with antagonistic activity being frequently described (Aerts et al., 2021; Glazebrook et al., 2003). In the current study, we uncovered the upregulation of JASMONATE ZIM (JAZ) domain protein genes *JAZ5* (*LOC115712145*) and *JAZ8* (*LOC115701213*) in response to infection with *S. sclerotiorum*. JAZ proteins act as transcriptional repressors of JA signalling through binding of MYC transcription factors (Guo et al., 2018). Low cellular levels of JA result in transcriptional repression of JA signalling, while increased JA levels lead to JAZ proteasomal degradation, allowing for transcription of JA-responsive genes (Howe, 2010; Pauwels & Goossens, 2011). In our dataset, with enrichment of *C. sativa* SA biosynthesis and upregulation of *PAL* activity at 3 and 5 dpi, it remains possible that JA signalling is being transcriptionally repressed at these timepoints, resulting from increasing endogenous SA levels arising from *S. sclerotiorum* infection. Quantification of endogenous hormone levels across the infection process could provide additional insight into the role of plant hormones in defense against necrotrophic fungal pathogens.

While PAL is known to be involved in lignification, it is also involved in SA biosynthesis in various plant species (Kim & Hwang, 2014; Ullah et al., 2023). SA biosynthesis is initiated during both ETI and PTI in response to recognition of PAMPs or pathogenic effectors (Mishina & Zeier, 2007). Increased SA levels are required for plant SAR initiation, which is accompanied and characterized by increased systemic PR gene expression (Pieterse et al., 2014). Belonging to the PR families PR-3, -4, -8, and -11, chitinases are among the most abundant PR proteins (Chouhan et al., 2023). Our dataset revealed the upregulation of chitinase genes across the *S.*

sclerotiorum infection process. While chitinase activity has yet to be described in pathogen interactions with *C. sativa*, previous work done *in vitro* has shown that *C. sativa* significantly increased chitinase levels in shoot tissue in response to chitosan treatment (Suwanchaikasem et al., 2023). In addition to the upregulation of chitinases, we also observed increases in gene activity of the PR-5 and PR-10 subfamilies. It is thought that PR-5 proteins exhibit antifungal activity by inserting themselves into fungal membranes to create a transmembrane pore, later leading to influx of water and subsequent fungal osmotic rupture (Sinha et al., 2014). Unlike the PR-5 proteins however, the function of PR-10 proteins remains largely unclear, which may be attributed to the large multi-gene families they code for (Fernandes et al., 2013; Sinha et al., 2014). Current studies have tied PR-10 proteins to cellular signalling cascades through the binding of hydrophobic ligands that include cytokinins, flavonoids, fatty acids and steroids (Fernandes et al., 2013), while others have reported that the proteins possess RNAse activity (Park et al., 2004). As our study serves as one of the first transcriptome-level investigations of the infection of *C. sativa* with any fungal pathogen, future studies that explore PR protein activity in other fungal interactions with *C. sativa* may reveal how PR gene expression may be engineered or selected to develop more resistant germplasm.

As complex specialized secondary plant metabolites, terpenes serve various purposes to plants that include attracting pollinators, attracting insect predators of feeding herbivores, and creating chemical and physical barriers to herbivorous and ovipositing insects, as well as invading pathogens (Chen et al., 2011; Keeling & Bohlmann, 2006). Specific to our study, we saw the upregulation of *(-)-GERMACRENE D SYNTHASE* in addition to several loci that encode *MONOTERPENE SYNTHASE 1 (MTS1* or *TPS1).* Previous studies have revealed that *TPS1* gene

expression (a form of *(-)-GERMACRENE D SYNTHASE*) and endogenous (-)-germacrene D levels were seen to increase in hybrid poplar (*Populus trichocarpa* x *deltoides*) in response to mechanical wounding (Arimura et al., 2004). Furthermore, research done in strawberry (*Fragaria × ananassa*) revealed that *TPS1* overexpression mutants capable of producing increased levels of germacrene-D displayed an increased resistance to the fungal necrotroph, *B. cinerea* (Zhang et al., 2022). In our study, we uncovered the downregulation of *(-)-LIMONENE SYNTHASE* in response to *S. sclerotiorum* infection. Although not explored in *C. sativa*, studies in *Citrus unshiu* (Satsuma mandarin) revealed that fruits deficient in D-limonene production were highly resistant to infection by the necrotrophic fungus, *Penicillium digitatum* (Rodríguez et al., 2014). Authors went as far as to describe D-limonene accumulation as essential for *P. digitatum* infection progression in *C. unshiu*. Currently, study of terpene synthase activity and accumulation in response to fungal pathogen attack has yet to be examined in *C. sativa.* As *C. sativa* terpenoid profiles often serve as a basis for modern selective breeding due to their impact on scent and flavour characteristics, further study is required to explore the impact that terpenes play in the *C. sativa* defense response. With varying terpenoid profiles attributed to unique *C. sativa* cultivars, the question arises of how different cultivars may respond to pathogen attack based on terpenoid profile composition; and whether selective breeding may allow for the production of cultivars that exhibit an increased resistance phenotype.

Taken together, this study provides a comprehensive investigation into the transcriptional and anatomical changes that occur as *S. sclerotiorum* initiates infection in the *C. sativa* inflorescence. Our data reveal large shifts in host gene activity in response to infection with *S. sclerotiorum* that largely peak at 5 dpi. Gene categories identified in *C. sativa* show complex

shifts in SA-JA hormone signalling and REDOX buffering associated with the plant defense responses across time post inoculation. Anatomical study revealed extensive degradation of host cortical and vascular phloem tissues associated with the production of fungal toxins and CWDEs. Additional studies conducting molecular and biochemical validation of the various gene products and metabolites identified throughout this study will allow for increased understanding of this pathosystem and can help to direct future crop improvement studies.

CHAPTER FIVE: Conclusions and future directions

In this study, we characterized the *C. sativa*-*S. sclerotiorum* pathosystem at the transcriptomic and anatomical levels. Using a dual mRNA-sequencing approach, we were able to explore gene expression in both the host plant as well as the fungal pathogen across time post inoculation. Additionally, a histological approach was used to examine the host-pathogen interface at the anatomical level across time. This work serves as the first detailed description of the *C. sativa*-*S. sclerotiorum* pathosystem at the cellular and molecular levels, acting as a foundation for further study of this pathosystem, and the interaction between *C. sativa* and other fungal pathogens. Through gene level analyses, this study provides a valuable resource that may be used for the development of novel crop protection tools to help protect *C. sativa* against devastating yield losses caused by fungal pathogens such as *S. sclerotiorum*.

Limited research has been conducted describing the molecular interaction between *C. sativa* and its pathogens due to years of legal constraints in studying this plant. This research is of value to other researchers interested in investigating the interaction between *C. sativa* and other fungal necrotrophs such as *B. cinerea.* While this study used mycelial plugs as an inoculant, future studies are required that use an ascospore-based approach ensure adequate representation of the various *S. sclerotiorum* infection styles plants may encounter in the field/commercial growing operations. Furthermore, additional studies investigating a larger cohort of *C. sativa* cultivars should provide insight into the diversity of defense pathways and possible innate resistance to *S. sclerotiorum*. While this study focused on genes involved in *S. sclerotiorum* resistance, targeting susceptibility genes across different *C. sativa* cultivars with

gene editing technologies such as CRISPR may allow for additional discovery surrounding resistance.

Given this work serves as a foundation for the description of the *C. sativa – S. sclerotiorum* pathosystem, there are a number of future directions ripe for experimental inquiry. One direct extension of this research would be to investigate transcription factors involved with the identified gene lists that respond to infection across time. As the coordinated shifts in gene expression associated with the plant defense response are largely controlled though transcription factor networks and their associated DNA binding sites, exploring transcription factor activity would help to increase the resolution of the transcriptional control and regulatory networks involved in defense gene expression. These additional insights into transcriptional regulation would not only provide further mechanistic insight into the underlying defense response pathways identified in this study but could also be used for the future development of crops that demonstrate a greater resistance to fungal pathogens. Future directions for this research also include exploring non-traditional-fungicide treatment options to protect *C. sativa* against necrotrophic pathogens. With strict limitations and mandatory analytical testing requirements set for fungicide MRLs in *C. sativa* taken to market, novel crop protection strategies for *C. sativa* are required. Foliar treatment options I would be interested in exploring include the application or boric acid or an RNA interference (RNAi) based strategy to help protect *C. sativa* against fungal infection. Previous work has shown that both boric acid and RNAi-based approaches have been efficacious in reducing *S. sclerotiorum* disease severity in species that include *B. napus* and *A. thaliana,* among others, suggesting a potential for successful application in *C. sativa* fungal pathosystems (Cale et al., 2024; McLoughlin et al., 2018; Walker et al., 2023; Wytinck et al.,

2022). The datasets generated in this study can serve as valuable tools for the identification of novel gene targets for fungal control. Through targeting genes essential for fungal pathogenicity at various stages throughout host infection, new fungal gene targets can be identified for use in spray-induced or host-induced gene silencing approaches. Without the current availability of commercial fungicides for use in *C. sativa*, these alternatives hold incredible promise in helping to fulfill the critical and immediate need for novel protection strategies to defend *C. sativa* against devastating fungal pathogens such as *S. sclerotiorum.*

The data generated in this study provide a framework in describing the interaction between *C. sativa* and *S. sclerotiorum* at the transcriptomic and cellular levels across time. Future studies focused on functional gene validation, transcriptional regulation and biochemical analysis will contribute to a more complete understanding of this pathosystem. Together with the dataset generated in our study, this work will serve as a resource for future researchers to design novel crop protection tools and establish breeding targets to help protect *C. sativa* against *S. sclerotiorum* and other necrotrophic fungal pathogens.

REFERENCES

Adal, A. M., Doshi, K., Holbrook, L., & Mahmoud, S. S. (2021). Comparative RNA-Seq analysis reveals genes associated with masculinization in female Cannabis sativa. *Planta*, *253*(1), 17. https://doi.org/10.1007/s00425-020-03522-y

Aerts, N., Pereira Mendes, M., & Van Wees, S. C. M. (2021). Multiple levels of crosstalk in hormone networks regulating plant defense. *The Plant Journal*, *105*(2), 489–504. https://doi.org/10.1111/tpj.15124

Alkooranee, J. T., Aledan, T. R., Ali, A. K., Lu, G., Zhang, X., Wu, J., Fu, C., & Li, M. (2017). Detecting the Hormonal Pathways in Oilseed Rape behind Induced Systemic Resistance by Trichoderma harzianum TH12 to Sclerotinia sclerotiorum. *PLOS ONE*, *12*(1), e0168850. https://doi.org/10.1371/journal.pone.0168850

Almagro, L., Gómez Ros, L. V., Belchi-Navarro, S., Bru, R., Ros Barceló, A., & Pedreño, M. A. (2009). Class III peroxidases in plant defence reactions. *Journal of Experimental Botany*, *60*(2), 377–390. https://doi.org/10.1093/jxb/ern277

Amselem, J., Cuomo, C. A., Kan, J. A. L. van, Viaud, M., Benito, E. P., Couloux, A., Coutinho, P. M., Vries, R. P. de, Dyer, P. S., Fillinger, S., Fournier, E., Gout, L., Hahn, M., Kohn, L., Lapalu, N., Plummer, K. M., Pradier, J.-M., Quévillon, E., Sharon, A., … Dickman, M. (2011). Genomic Analysis of the Necrotrophic Fungal Pathogens Sclerotinia sclerotiorum and Botrytis cinerea. *PLOS Genetics*, *7*(8), e1002230. https://doi.org/10.1371/journal.pgen.1002230

Anders, S., & Huber, W. (2010). Differential expression analysis for sequence count data. *Genome Biology*, *11*(10), R106. https://doi.org/10.1186/gb-2010-11-10-r106

Andrews, S. (2010, April). *FastQC A Quality Control tool for High Throughput Sequence Data*. https://www.bioinformatics.babraham.ac.uk/projects/fastqc/

Arimura, G., Huber, D. P. W., & Bohlmann, J. (2004). Forest tent caterpillars (Malacosoma disstria) induce local and systemic diurnal emissions of terpenoid volatiles in hybrid poplar (Populus trichocarpa × deltoides): cDNA cloning, functional characterization, and patterns of gene expression of (−)-germacrene D synthase, PtdTPS1. *The Plant Journal*, *37*(4), 603–616. https://doi.org/10.1111/j.1365-313X.2003.01987.x

Bains, P. S., Bennypaul, H. S., Blade, S. F., & Weeks, C. (2000). First Report of Hemp Canker Caused by Sclerotinia sclerotiorum in Alberta, Canada. *Plant Disease*, *84*(3), 372–372. https://doi.org/10.1094/PDIS.2000.84.3.372B

Balthazar, C., Cantin, G., Novinscak, A., Joly, D. L., & Filion, M. (2020). Expression of Putative Defense Responses in Cannabis Primed by Pseudomonas and/or Bacillus Strains and Infected by Botrytis cinerea. *Frontiers in Plant Science*, *11*. https://www.frontiersin.org/articles/10.3389/fpls.2020.572112

Becker, M. G., Walker, P. L., Pulgar-Vidal, N. C., & Belmonte, M. F. (2017). SeqEnrich: A tool to predict transcription factor networks from co-expressed Arabidopsis and Brassica napus gene sets. *PLOS ONE*, *12*(6), e0178256. https://doi.org/10.1371/journal.pone.0178256

Bellincampi, D., Cervone, F., & Lionetti, V. (2014). Plant cell wall dynamics and wall-related susceptibility in plant–pathogen interactions. *Frontiers in Plant Science*, *5*. https://doi.org/10.3389/fpls.2014.00228

Benjamini, Y., & Hochberg, Y. (1995). Controlling the False Discovery Rate: A Practical and Powerful Approach to Multiple Testing. *Journal of the Royal Statistical Society. Series B (Methodological)*, *57*(1), 289–300.

Bernsdorff, F., Döring, A.-C., Gruner, K., Schuck, S., Bräutigam, A., & Zeier, J. (2016). Pipecolic Acid Orchestrates Plant Systemic Acquired Resistance and Defense Priming via Salicylic Acid-Dependent and -Independent Pathways. *The Plant Cell*, *28*(1), 102–129. https://doi.org/10.1105/tpc.15.00496

Bolton, M. D., Thomma, B. P. H. J., & Nelson, B. D. (2006). Sclerotinia sclerotiorum (Lib.) de Bary: Biology and molecular traits of a cosmopolitan pathogen. *Molecular Plant Pathology*, *7*(1), 1–16. https://doi.org/10.1111/j.1364-3703.2005.00316.x

Booth, J. K., & Bohlmann, J. (2019). Terpenes in *Cannabis sativa* – From plant genome to humans. *Plant Science*, *284*, 67–72. https://doi.org/10.1016/j.plantsci.2019.03.022

Booth, J. K., Page, J. E., & Bohlmann, J. (2017). Terpene synthases from Cannabis sativa. *PLoS ONE*, *12*(3), e0173911. https://doi.org/10.1371/journal.pone.0173911

Bot, P., Mun, B.-G., Imran, Q. M., Hussain, A., Lee, S.-U., Loake, G., & Yun, B.-W. (2019). Differential expression of AtWAKL10 in response to nitric oxide suggests a putative role in biotic and abiotic stress responses. *PeerJ*, *7*, e7383. https://doi.org/10.7717/peerj.7383

Braich, S., Baillie, R. C., Jewell, L. S., Spangenberg, G. C., & Cogan, N. O. I. (2019). Generation of a Comprehensive Transcriptome Atlas and Transcriptome Dynamics in Medicinal Cannabis. *Scientific Reports*, *9*(1), Article 1. https://doi.org/10.1038/s41598-019-53023-6

Brutus, A., Sicilia, F., Macone, A., Cervone, F., & De Lorenzo, G. (2010). A domain swap approach reveals a role of the plant wall-associated kinase 1 (WAK1) as a receptor of

oligogalacturonides. *Proceedings of the National Academy of Sciences*, *107*(20), 9452–9457. https://doi.org/10.1073/pnas.1000675107

Cale, N. L., Walker, P. L., Sankar, S., Robertson, S. M., Wilkins, O., & Belmonte, M. F. (2024). Global mRNA profiling reveals the effect of boron as a crop protection tool against Sclerotinia sclerotiorum. *AoB PLANTS*, plae056. https://doi.org/10.1093/aobpla/plae056

Calla, B., Blahut-Beatty, L., Koziol, L., Zhang, Y., Neece, D. J., Carbajulca, D., Garcia, A., Simmonds, D. H., & Clough, S. J. (2014). Genomic evaluation of oxalate-degrading transgenic soybean in response to Sclerotinia sclerotiorum infection. *Molecular Plant Pathology*, *15*(6), 563–575. https://doi.org/10.1111/mpp.12115

Cessna, S. G., Sears, V. E., Dickman, M. B., & Low, P. S. (2000). Oxalic Acid, a Pathogenicity Factor for Sclerotinia sclerotiorum, Suppresses the Oxidative Burst of the Host Plant. *The Plant Cell*, *12*(11), 2191–2199. https://doi.org/10.2307/3871114

Chan, A., & Belmonte, M. F. (2013). Histological and ultrastructural changes in canola (Brassica napus) funicular anatomy during the seed lifecycle. *Botany*, *91*(10), 671–679. https://doi.org/10.1139/cjb-2013-0141

Chen, F., Tholl, D., Bohlmann, J., & Pichersky, E. (2011). The family of terpene synthases in plants: A mid-size family of genes for specialized metabolism that is highly diversified throughout the kingdom. *The Plant Journal*, *66*(1), 212–229. https://doi.org/10.1111/j.1365-313X.2011.04520.x

Chouhan, R., Ahmed, S., & Gandhi, S. G. (2023). Over-expression of PR proteins with chitinase activity in transgenic plants for alleviation of fungal pathogenesis. *Journal of Plant Pathology*, *105*(1), 69–81. https://doi.org/10.1007/s42161-022-01226-8

Craven, C. B., Wawryk, N., Jiang, P., Liu, Z., & Li, X.-F. (2019). Pesticides and trace elements in cannabis: Analytical and environmental challenges and opportunities. *Journal of Environmental Sciences*, *85*, 82–93. https://doi.org/10.1016/j.jes.2019.04.028

Davidson, A. L., Blahut-Beatty, L., Itaya, A., Zhang, Y., Zheng, S., & Simmonds, D. (2016). Histopathology of Sclerotinia sclerotiorum infection and oxalic acid function in susceptible and resistant soybean. *Plant Pathology*, *65*(6), 878–887. https://doi.org/10.1111/ppa.12514

de Meijer, E. P. M., Bagatta, M., Carboni, A., Crucitti, P., Moliterni, V. M. C., Ranalli, P., & Mandolino, G. (2003). The Inheritance of Chemical Phenotype in Cannabis sativa L. *Genetics*, *163*(1), 335–346. https://doi.org/10.1093/genetics/163.1.335

Derbyshire, M. C., & Denton-Giles, M. (2016). The control of sclerotinia stem rot on oilseed rape (Brassica napus): Current practices and future opportunities. *Plant Pathology*, *65*(6), 859–877. https://doi.org/10.1111/ppa.12517

Dickman, M. B., Park, Y. K., Oltersdorf, T., Li, W., Clemente, T., & French, R. (2001). Abrogation of disease development in plants expressing animal antiapoptotic genes. *Proceedings of the National Academy of Sciences*, *98*(12), 6957–6962. https://doi.org/10.1073/pnas.091108998

Divashuk, M. G., Alexandrov, O. S., Razumova, O. V., Kirov, I. V., & Karlov, G. I. (2014). Molecular Cytogenetic Characterization of the Dioecious Cannabis sativa with an XY Chromosome Sex Determination System. *PLOS ONE*, *9*(1), e85118. https://doi.org/10.1371/journal.pone.0085118

Dodds, P. N., Chen, J., & Outram, M. A. (2024). Pathogen perception and signaling in plant immunity. *The Plant Cell*, koae020. https://doi.org/10.1093/plcell/koae020

Duke, K. A., Becker, M. G., Girard, I. J., Millar, J. L., Dilantha Fernando, W. G., Belmonte, M. F., & de Kievit, T. R. (2017). The biocontrol agent Pseudomonas chlororaphis PA23 primes Brassica napus defenses through distinct gene networks. *BMC Genomics*, *18*(1), 467. https://doi.org/10.1186/s12864-017-3848-6

Ekins, M. G., Aitken, E. A. B., & Goulter, K. C. (2002). Carpogenic germination of Sclerotinia minor and potential distribution in Australia. *Australasian Plant Pathology*, *31*(3), 259–265. https://doi.org/10.1071/AP02022

Fernandes, H., Michalska, K., Sikorski, M., & Jaskolski, M. (2013). Structural and functional aspects of PR-10 proteins. *The FEBS Journal*, *280*(5), 1169–1199. https://doi.org/10.1111/febs.12114

Fischedick, J. T. (2017). Identification of Terpenoid Chemotypes Among High (−)-trans-Δ9-Tetrahydrocannabinol-Producing Cannabis sativa L. Cultivars. *Cannabis and Cannabinoid Research*, *2*(1), 34–47. https://doi.org/10.1089/can.2016.0040

Garfinkel, A. R. (2021). First Report of Sclerotinia sclerotiorum Causing Stem Canker on Cannabis sativa in Oregon. *Plant Disease*, *105*(8), 2245. https://doi.org/10.1094/PDIS-10-20-2142-PDN

Girard, I. J., Tong, C., Becker, M. G., Mao, X., Huang, J., de Kievit, T., Fernando, W. G. D., Liu, S., & Belmonte, M. F. (2017). RNA sequencing of Brassica napus reveals cellular redox control of Sclerotinia infection. *Journal of Experimental Botany*, *68*(18), 5079–5091. https://doi.org/10.1093/jxb/erx338

Glazebrook, J., Chen, W., Estes, B., Chang, H.-S., Nawrath, C., Métraux, J.-P., Zhu, T., & Katagiri, F. (2003). Topology of the network integrating salicylate and jasmonate signal

transduction derived from global expression phenotyping. *The Plant Journal*, *34*(2), 217–228. https://doi.org/10.1046/j.1365-313X.2003.01717.x

Godoy, G., Steadman, J. R., Dickman, M. B., & Dam, R. (1990). Use of mutants to demonstrate the role of oxalic acid in pathogenicity of *Sclerotinia sclerotiorum* on *Phaseolus vulgaris*. *Physiological and Molecular Plant Pathology*, *37*(3), 179–191. https://doi.org/10.1016/0885-5765(90)90010-U

Goldman, S., Bramante, J., Vrdoljak, G., Guo, W., Wang, Y., Marjanovic, O., Orlowicz, S., Di Lorenzo, R., & Noestheden, M. (2021). The analytical landscape of cannabis compliance testing. *Journal of Liquid Chromatography & Related Technologies*, *44*(9–10), 403–420. https://doi.org/10.1080/10826076.2021.1996390

Government of Canada. (2018, June 27). *Consolidated federal laws of Canada, Cannabis Regulations*. https://laws-lois.justice.gc.ca/eng/regulations/SOR-2018-144/FullText.html

Government of Canada. (2024, September 12). *Licensed area market data* [Statistics]. https://www.canada.ca/en/health-canada/services/drugs-medication/cannabis/research-data/market/licensed-area.html

Govrin, E. M., & Levine, A. (2000). The hypersensitive response facilitates plant infection by the necrotrophic pathogen Botrytis cinerea. *Current Biology*, *10*(13), 751–757. https://doi.org/10.1016/S0960-9822(00)00560-1

Guo, Q., Yoshida, Y., Major, I. T., Wang, K., Sugimoto, K., Kapali, G., Havko, N. E., Benning, C., & Howe, G. A. (2018). JAZ repressors of metabolic defense promote growth and reproductive fitness in Arabidopsis. *Proceedings of the National Academy of Sciences*, *115*(45), E10768–E10777. https://doi.org/10.1073/pnas.1811828115

Hammond, D., Goodman, S., Wadsworth, E., Rynard, V., Boudreau, C., & Hall, W. (2020). Evaluating the impacts of cannabis legalization: The International Cannabis Policy Study. *International Journal of Drug Policy*, *77*, 102698. https://doi.org/10.1016/j.drugpo.2020.102698

Harvey, A., van den Berg, N., & Swart, V. (2024). Describing and characterizing the WAK/WAKL gene family across plant species: A systematic review. *Frontiers in Plant Science*, *15*. https://doi.org/10.3389/fpls.2024.1467148

He, Z.-H., He, D., & Kohorn, B. D. (1998). Requirement for the induced expression of a cell wall associated receptor kinase for survival during the pathogen response. *The Plant Journal*, *14*(1), 55–63. https://doi.org/10.1046/j.1365-313X.1998.00092.x

Hegedus, D. D., & Rimmer, S. R. (2005). Sclerotinia sclerotiorum: When "to be or not to be" a pathogen? *FEMS Microbiology Letters*, *251*(2), 177–184. https://doi.org/10.1016/j.femsle.2005.07.040

Hillig, K. W. (2005). Genetic evidence for speciation in Cannabis (Cannabaceae). *Genetic Resources and Crop Evolution*, *52*(2), 161–180. https://doi.org/10.1007/s10722-003-4452-y

Horbach, R., Navarro-Quesada, A. R., Knogge, W., & Deising, H. B. (2011). When and how to kill a plant cell: Infection strategies of plant pathogenic fungi. *Journal of Plant Physiology*, *168*(1), 51–62. https://doi.org/10.1016/j.jplph.2010.06.014

Hossain, M. M., Sultana, F., Li, W., Tran, L.-S. P., & Mostofa, M. G. (2023). Sclerotinia sclerotiorum (Lib.) de Bary: Insights into the Pathogenomic Features of a Global Pathogen. *Cells*, *12*(7), Article 7. https://doi.org/10.3390/cells12071063

Howe, G. A. (2010). Ubiquitin Ligase-Coupled Receptors Extend Their Reach to Jasmonate. *Plant Physiology*, *154*(2), 471–474. https://doi.org/10.1104/pp.110.161190

Huang, Y., Li, D., Zhao, L., Chen, A., Li, J., Tang, H., Pan, G., Chang, L., Deng, Y., & Huang, S. (2019). Comparative transcriptome combined with physiological analyses revealed key factors for differential cadmium tolerance in two contrasting hemp (*Cannabis sativa* L.) cultivars. *Industrial Crops and Products*, *140*, 111638. https://doi.org/10.1016/j.indcrop.2019.111638

Hurgobin, B., Tamiru-Oli, M., Welling, M. T., Doblin, M. S., Bacic, A., Whelan, J., & Lewsey, M. G. (2021). Recent advances in Cannabis sativa genomics research. *New Phytologist*, *230*(1), 73–89. https://doi.org/10.1111/nph.17140

Jung, H. W., Tschaplinski, T. J., Wang, L., Glazebrook, J., & Greenberg, J. T. (2009). Priming in Systemic Plant Immunity. *Science*, *324*(5923), 89–91. https://doi.org/10.1126/science.1170025

Kabbage, M., Yarden, O., & Dickman, M. B. (2015). Pathogenic attributes of *Sclerotinia sclerotiorum*: Switching from a biotrophic to necrotrophic lifestyle. *Plant Science*, *233*, 53–60. https://doi.org/10.1016/j.plantsci.2014.12.018

Keeling, C. I., & Bohlmann, J. (2006). Genes, enzymes and chemicals of terpenoid diversity in the constitutive and induced defence of conifers against insects and pathogens. *New Phytologist*, *170*(4), 657–675. https://doi.org/10.1111/j.1469-8137.2006.01716.x

Kim, D., Paggi, J. M., Park, C., Bennett, C., & Salzberg, S. L. (2019). Graph-based genome alignment and genotyping with HISAT2 and HISAT-genotype. *Nature Biotechnology*, *37*(8), Article 8. https://doi.org/10.1038/s41587-019-0201-4

Kim, D. S., & Hwang, B. K. (2014). An important role of the pepper phenylalanine ammonia-lyase gene (PAL1) in salicylic acid-dependent signalling of the defence response to microbial pathogens. *Journal of Experimental Botany*, *65*(9), 2295–2306. https://doi.org/10.1093/jxb/eru109

Kim, K. S., Min, J.-Y., & Dickman, M. B. (2008). Oxalic Acid Is an Elicitor of Plant Programmed Cell Death during *Sclerotinia sclerotiorum* Disease Development. *Molecular Plant-Microbe Interactions®*, *21*(5), 605–612. https://doi.org/10.1094/MPMI-21-5-0605

Kohorn, B. D., & Kohorn, S. L. (2012). The cell wall-associated kinases, WAKs, as pectin receptors. *Frontiers in Plant Science*, *3*. https://doi.org/10.3389/fpls.2012.00088

Lamb, C., & Dixon, R. A. (1997). THE OXIDATIVE BURST IN PLANT DISEASE RESISTANCE. *Annual Review of Plant Biology*, *48*(Volume 48, 1997), 251–275. https://doi.org/10.1146/annurev.arplant.48.1.251

Lemay, J., Zheng, Y., & Scott-Dupree, C. (2022). Factors Influencing the Efficacy of Biological Control Agents Used to Manage Insect Pests in Indoor Cannabis (Cannabis sativa) Cultivation. *Frontiers in Agronomy*, *4*. https://doi.org/10.3389/fagro.2022.795989

Leme, F. M., Schönenberger, J., Staedler, Y. M., & Teixeira, S. P. (2020). Comparative floral development reveals novel aspects of structure and diversity of flowers in Cannabaceae. *Botanical Journal of the Linnean Society*, *193*(1), 64–83. https://doi.org/10.1093/botlinnean/boaa004

Liang, X., & Rollins, J. A. (2018). Mechanisms of Broad Host Range Necrotrophic Pathogenesis in Sclerotinia sclerotiorum. *Phytopathology®*, *108*(10), 1128–1140. https://doi.org/10.1094/PHYTO-06-18-0197-RVW

Liao, Y., Smyth, G. K., & Shi, W. (2014). featureCounts: An efficient general purpose program for assigning sequence reads to genomic features. *Bioinformatics*, *30*(7), 923–930. https://doi.org/10.1093/bioinformatics/btt656

Lim, J. D. (2023). *Cannabis sativa Isolate KNU-18-1 (Cultivar: Pink Pepper), Whole Genome Sequencing Project* [Dataset]. Genbank.

Liu, J., Qiao, Q., Cheng, X., Du, G., Deng, G., Zhao, M., & Liu, F. (2016). Transcriptome differences between fiber-type and seed-type Cannabis sativa variety exposed to salinity. *Physiology and Molecular Biology of Plants*, *22*(4), 429–443. https://doi.org/10.1007/s12298-016-0381-z

Long, T., Wagner, M., Demske, D., Leipe, C., & Tarasov, P. E. (2017). Cannabis in Eurasia: Origin of human use and Bronze Age trans-continental connections. *Vegetation History and Archaeobotany*, *26*(2), 245–258. https://doi.org/10.1007/s00334-016-0579-6

Love, M. I., Huber, W., & Anders, S. (2014). Moderated estimation of fold change and dispersion for RNA-seq data with DESeq2. *Genome Biology*, *15*(12), 550. https://doi.org/10.1186/s13059-014-0550-8

Lumsden, R. D. (1976). Pectolytic enzymes of *Sclerotinia sclerotiorum* and their localization in infected bean. *Canadian Journal of Botany*, *54*(23), 2630–2641. https://doi.org/10.1139/b76-283

McLoughlin, A. G., Wytinck, N., Walker, P. L., Girard, I. J., Rashid, K. Y., de Kievit, T., Fernando, W. G. D., Whyard, S., & Belmonte, M. F. (2018). Identification and application of exogenous dsRNA confers plant protection against Sclerotinia sclerotiorum and Botrytis cinerea. *Scientific Reports*, *8*(1), 7320. https://doi.org/10.1038/s41598-018-25434-4

Mishina, T. E., & Zeier, J. (2007). Pathogen-associated molecular pattern recognition rather than development of tissue necrosis contributes to bacterial induction of systemic acquired resistance in Arabidopsis. *The Plant Journal*, *50*(3), 500–513. https://doi.org/10.1111/j.1365-313X.2007.03067.x

Monthony, A. S., de Ronne, M., & Torkamaneh, D. (2024). Exploring ethylene-related genes in Cannabis sativa: Implications for sexual plasticity. *Plant Reproduction*, *37*(3), 321–339. https://doi.org/10.1007/s00497-023-00492-5

Park, C.-J., Kim, K.-J., Shin, R., Park, J. M., Shin, Y.-C., & Paek, K.-H. (2004). Pathogenesis-related protein 10 isolated from hot pepper functions as a ribonuclease in an antiviral pathway. *The Plant Journal*, *37*(2), 186–198. https://doi.org/10.1046/j.1365-313X.2003.01951.x

Pauwels, L., & Goossens, A. (2011). The JAZ Proteins: A Crucial Interface in the Jasmonate Signaling Cascade. *The Plant Cell*, *23*(9), 3089–3100. https://doi.org/10.1105/tpc.111.089300

Pieterse, C. M. J., Zamioudis, C., Berendsen, R. L., Weller, D. M., Van Wees, S. C. M., & Bakker, P. A. H. M. (2014). Induced Systemic Resistance by Beneficial Microbes. *Annual Review of Phytopathology*, *52*(1), 347–375. https://doi.org/10.1146/annurev-phyto-082712-102340

Prentout, D., Razumova, O., Rhoné, B., Badouin, H., Henri, H., Feng, C., Käfer, J., Karlov, G., & Marais, G. A. B. (2020). An efficient RNA-seq-based segregation analysis identifies the sex chromosomes of Cannabis sativa. *Genome Research*, *30*(2), 164–172. https://doi.org/10.1101/gr.251207.119

Pruitt, R. N., Gust, A. A., & Nürnberger, T. (2021). Plant immunity unified. *Nature Plants*, *7*(4), Article 4. https://doi.org/10.1038/s41477-021-00903-3

Punja, Z. K. (2021). Emerging diseases of Cannabis sativa and sustainable management. *Pest Management Science*, *77*(9), 3857–3870. https://doi.org/10.1002/ps.6307

Punja, Z. K., & Ni, L. (2021). The bud rot pathogens infecting cannabis (Cannabis sativa L., marijuana) inflorescences: Symptomology, species identification, pathogenicity and biological control. *Canadian Journal of Plant Pathology*, *43*(6), 827–854. https://doi.org/10.1080/07060661.2021.1936650

Purdy, L. H. (1979). Sclerotinia sclerotiorum: History, diseases and symptomatology, host range, geographic distribution, and impact. *Phytopathology*, *69*(8), 875-880.

R Core Team. (2021). *R: A language and environment for statistical computing*. R Foundation for Statistical Computing, Vienna, Austria. URL https://www.R-project.org/

Raman, V., Lata, H., Chandra, S., Khan, I. A., & ElSohly, M. A. (2017). Morpho-Anatomy of Marijuana (Cannabis sativa L.). In S. Chandra, H. Lata, & M. A. ElSohly (Eds.), *Cannabis sativa L. - Botany and Biotechnology* (pp. 123–136). Springer International Publishing. https://doi.org/10.1007/978-3-319-54564-6_5

Ren, G., Zhang, X., Li, Y., Ridout, K., Serrano-Serrano, M. L., Yang, Y., Liu, A., Ravikanth, G., Nawaz, M. A., Mumtaz, A. S., Salamin, N., & Fumagalli, L. (2021). Large-scale whole-genome resequencing unravels the domestication history of Cannabis sativa. *Science Advances*, *7*(29), eabg2286. https://doi.org/10.1126/sciadv.abg2286

Rodríguez, A., Shimada, T., Cervera, M., Alquézar, B., Gadea, J., Gómez-Cadenas, A., De Ollas, C. J., Rodrigo, M. J., Zacarías, L., & Peña, L. (2014). Terpene Down-Regulation Triggers

Defense Responses in Transgenic Orange Leading to Resistance against Fungal Pathogens. *Plant Physiology*, *164*(1), 321–339. https://doi.org/10.1104/pp.113.224279

Rodziewicz, P., Loroch, S., Marczak, Ł., Sickmann, A., & Kayser, O. (2019). Cannabinoid synthases and osmoprotective metabolites accumulate in the exudates of *Cannabis sativa* L. glandular trichomes. *Plant Science*, *284*, 108–116. https://doi.org/10.1016/j.plantsci.2019.04.008

Rossi, F. R., Krapp, A. R., Bisaro, F., Maiale, S. J., Pieckenstain, F. L., & Carrillo, N. (2017). Reactive oxygen species generated in chloroplasts contribute to tobacco leaf infection by the necrotrophic fungus Botrytis cinerea. *The Plant Journal*, *92*(5), 761–773. https://doi.org/10.1111/tpj.13718

Saharan, G. S., & Mehta, N. (2008). *Sclerotinia Diseases of Crop Plants: Biology, Ecology and Disease Management*. Springer Science & Business Media.

Sandler, L. N., Beckerman, J. L., Whitford, F., & Gibson, K. A. (2019). *Cannabis* as conundrum. *Crop Protection*, *117*, 37–44. https://doi.org/10.1016/j.cropro.2018.11.003

Sasaki, K., Iwai, T., Hiraga, S., Kuroda, K., Seo, S., Mitsuhara, I., Miyasaka, A., Iwano, M., Ito, H., Matsui, H., & Ohashi, Y. (2004). Ten Rice Peroxidases Redundantly Respond to Multiple Stresses Including Infection with Rice Blast Fungus. *Plant and Cell Physiology*, *45*(10), 1442–1452. https://doi.org/10.1093/pcp/pch165

Sawler, J., Stout, J. M., Gardner, K. M., Hudson, D., Vidmar, J., Butler, L., Page, J. E., & Myles, S. (2015). The Genetic Structure of Marijuana and Hemp. *PLOS ONE*, *10*(8), e0133292. https://doi.org/10.1371/journal.pone.0133292

Seifbarghi, S., Borhan, M. H., Wei, Y., Coutu, C., Robinson, S. J., & Hegedus, D. D. (2017). Changes in the Sclerotinia sclerotiorum transcriptome during infection of Brassica napus. *BMC Genomics*, *18*(1), 266. https://doi.org/10.1186/s12864-017-3642-5

Sinha, M., Singh, R. P., Kushwaha, G. S., Iqbal, N., Singh, A., Kaushik, S., Kaur, P., Sharma, S., & Singh, T. P. (2014). Current Overview of Allergens of Plant Pathogenesis Related Protein Families. *The Scientific World Journal*, *2014*, 543195. https://doi.org/10.1155/2014/543195

Sirangelo, T. M., Ludlow, R. A., & Spadafora, N. D. (2023). Molecular Mechanisms Underlying Potential Pathogen Resistance in Cannabis sativa. *Plants*, *12*(15), 2764. https://doi.org/10.3390/plants12152764

Small, E. (2015). Evolution and Classification of Cannabis sativa (Marijuana, Hemp) in Relation to Human Utilization. *The Botanical Review*, *81*(3), 189–294. https://doi.org/10.1007/s12229-015-9157-3

Smolińska, U., & Kowalska, B. (2018). Biological control of the soil-borne fungal pathogen Sclerotinia sclerotiorum — a review. *Journal of Plant Pathology*, *100*(1), 1–12. https://doi.org/10.1007/s42161-018-0023-0

Song, W., Forderer, A., Yu, D., & Chai, J. (2021). Structural biology of plant defence. *New Phytologist*, *229*(2), 692–711. https://doi.org/10.1111/nph.16906

Stephens, C., Hammond-Kosack, K. E., & Kanyuka, K. (2022). WAKsing plant immunity, waning diseases. *Journal of Experimental Botany*, *73*(1), 22–37. https://doi.org/10.1093/jxb/erab422

Stephens, M. (2017). False discovery rates: A new deal. *Biostatistics*, *18*(2), 275–294. https://doi.org/10.1093/biostatistics/kxw041

Sutton, D. C., & Deverall, B. J. (1983). Studies on infection of bean (Phaseolus vulgaris) and soybean (Glycine max) by ascospores of Sclerotinia sclerotiarum. *Plant Pathology*, *32*(3), 251–261. https://doi.org/10.1111/j.1365-3059.1983.tb02832.x

Suwanchaikasem, P., Nie, S., Idnurm, A., Selby-Pham, J., Walker, R., & Boughton, B. A. (2023). Effects of chitin and chitosan on root growth, biochemical defense response and exudate proteome of Cannabis sativa. *Plant-Environment Interactions*, *4*(3), 115–133. https://doi.org/10.1002/pei3.10106

Thiessen, L. D., Schappe, T., Cochran, S., Hicks, K., & Post, A. R. (2020). Surveying for Potential Diseases and Abiotic Disorders of Industrial Hemp (Cannabis sativa) Production. *Plant Health Progress*, *21*(4), 321–332. https://doi.org/10.1094/PHP-03-20-0017-RS

Thomma, B. P., Penninckx, I. A., Cammue, B. P., & Broekaert, W. F. (2001). The complexity of disease signaling in *Arabidopsis*. *Current Opinion in Immunology*, *13*(1), 63–68. https://doi.org/10.1016/S0952-7915(00)00183-7

Ullah, C., Chen, Y.-H., Ortega, M. A., & Tsai, C.-J. (2023). The diversity of salicylic acid biosynthesis and defense signaling in plants: Knowledge gaps and future opportunities. *Current Opinion in Plant Biology*, *72*, 102349. https://doi.org/10.1016/j.pbi.2023.102349

Uloth, M. B., Clode, P. L., You, M. P., & Barbetti, M. J. (2016). Attack modes and defence reactions in pathosystems involving Sclerotinia sclerotiorum, Brassica carinata, B. juncea and B. napus. *Annals of Botany*, *117*(1), 79–95. https://doi.org/10.1093/aob/mcv150

van Bakel, H., Stout, J. M., Cote, A. G., Tallon, C. M., Sharpe, A. G., Hughes, T. R., & Page, J. E. (2011). The draft genome and transcriptome of Cannabis sativa. *Genome Biology*, *12*(10), R102. https://doi.org/10.1186/gb-2011-12-10-r102

van Loon, L. C., Rep, M., & Pieterse, C. M. J. (2006). Significance of Inducible Defense-related Proteins in Infected Plants. *Annual Review of Phytopathology*, *44*(Volume 44, 2006), 135–162. https://doi.org/10.1146/annurev.phyto.44.070505.143425

Walker, P. L., Girard, I. J., Becker, M. G., Giesbrecht, S., Whyard, S., Fernando, W. G. D., de Kievit, T. R., & Belmonte, M. F. (2022). Tissue-specific mRNA profiling of the Brassica napus–Sclerotinia sclerotiorum interaction uncovers novel regulators of plant immunity. *Journal of Experimental Botany*, *73*(19), 6697–6710. https://doi.org/10.1093/jxb/erac333

Walker, P. L., Ziegler, D. J., Giesbrecht, S., McLoughlin, A., Wan, J., Khan, D., Hoi, V., Whyard, S., & Belmonte, M. F. (2023). Control of white mold (Sclerotinia sclerotiorum) through plant-mediated RNA interference. *Scientific Reports*, *13*(1), 6477. https://doi.org/10.1038/s41598-023-33335-4

Wang, J., Zhang, Z., & Huang, R. (2013). Regulation of ascorbic acid synthesis in plants. *Plant Signaling & Behavior*, *8*(6), e24536. https://doi.org/10.4161/psb.24536

Wickham, H. (2011). Ggplot2. *WIREs Computational Statistics*, *3*(2), 180–185. https://doi.org/10.1002/wics.147

Willbur, J., McCaghey, M., Kabbage, M., & Smith, D. L. (2019). An overview of the Sclerotinia sclerotiorum pathosystem in soybean: Impact, fungal biology, and current management strategies. *Tropical Plant Pathology*, *44*(1), 3–11. https://doi.org/10.1007/s40858-018-0250-0

Williams, B., Kabbage, M., Kim, H.-J., Britt, R., & Dickman, M. B. (2011). Tipping the Balance: Sclerotinia sclerotiorum Secreted Oxalic Acid Suppresses Host Defenses by Manipulating the Host Redox Environment. *PLOS Pathogens*, *7*(6), e1002107. https://doi.org/10.1371/journal.ppat.1002107

Wojtaszek, P. (1997). Oxidative burst: An early plant response to pathogen infection. *Biochemical Journal*, *322*(3), 681–692. https://doi.org/10.1042/bj3220681

Wu, J., Zhao, Q., Yang, Q., Liu, H., Li, Q., Yi, X., Cheng, Y., Guo, L., Fan, C., & Zhou, Y. (2016). Comparative transcriptomic analysis uncovers the complex genetic network for resistance to Sclerotinia sclerotiorum in Brassica napus. *Scientific Reports*, *6*(1), Article 1. https://doi.org/10.1038/srep19007

Wytinck, N., Ziegler, D. J., Walker, P. L., Sullivan, D. S., Biggar, K. T., Khan, D., Sakariyahu, S. K., Wilkins, O., Whyard, S., & Belmonte, M. F. (2022). Host induced gene silencing of the Sclerotinia sclerotiorum ABHYDROLASE-3 gene reduces disease severity in Brassica napus. *PLOS ONE*, *17*(8), e0261102. https://doi.org/10.1371/journal.pone.0261102

Xie, Z., Mi, Y., Kong, L., Gao, M., Chen, S., Chen, W., Meng, X., Sun, W., Chen, S., & Xu, Z. (2023). Cannabis sativa: Origin and history, glandular trichome development, and cannabinoid biosynthesis. *Horticulture Research*, *10*(9), uhad150. https://doi.org/10.1093/hr/uhad150

Yan, W., Hu, P., Ni, Y., Zhao, H., Liu, X., Cao, H., Jia, M., Tian, B., Miao, H., & Liu, H. (2023). Genome-wide characterization of the wall-associated kinase-like (WAKL) family in sesame (Sesamum indicum) identifies a SiWAKL6 gene involved in resistance to Macrophomina Phaseolina. *BMC Plant Biology*, *23*(1), 624. https://doi.org/10.1186/s12870-023-04658-1

Yang, X., Justice, A., & Colburn, C. (2023). First report of Sclerotinia sclerotiorum causing stem canker on industrial hemp in South Carolina, USA. *Plant Disease*. https://doi.org/10.1094/PDIS-04-23-0700-PDN

Yeo, H. C., Reddy, V. A., Mun, B.-G., Leong, S. H., Dhandapani, S., Rajani, S., & Jang, I.-C. (2022). Comparative Transcriptome Analysis Reveals Coordinated Transcriptional Regulation of Central and Secondary Metabolism in the Trichomes of Cannabis Cultivars. *International Journal of Molecular Sciences*, *23*(15), Article 15. https://doi.org/10.3390/ijms23158310

Zeier, J. (2021). Metabolic regulation of systemic acquired resistance. *Current Opinion in Plant Biology*, *62*, 102050. https://doi.org/10.1016/j.pbi.2021.102050

Zhang, J., Zhang, C., Huang, S., Chang, L., Li, J., Tang, H., Dey, S., Biswas, A., Du, D., Li, D., & Zhao, L. (2021). Key Cannabis Salt-Responsive Genes and Pathways Revealed by Comparative Transcriptome and Physiological Analyses of Contrasting Varieties. *Agronomy*, *11*(11), Article 11. https://doi.org/10.3390/agronomy11112338

Zhang, M., Anderson, S. L., Brym, Z. T., & Pearson, B. J. (2021). Photoperiodic Flowering Response of Essential Oil, Grain, and Fiber Hemp (Cannabis sativa L.) Cultivars. *Frontiers in Plant Science*, *12*. https://www.frontiersin.org/articles/10.3389/fpls.2021.694153

Zhang, Z., Lu, S., Yu, W., Ehsan, S., Zhang, Y., Jia, H., & Fang, J. (2022). Jasmonate increases terpene synthase expression, leading to strawberry resistance to Botrytis cinerea infection. *Plant Cell Reports*, *41*(5), 1243–1260. https://doi.org/10.1007/s00299-022-02854-1